DOI: 10.1002/anie.201402780

Graphene

Chemistry with Graphene and Graphene Oxide—Challenges for Synthetic Chemists

Siegfried Eigler and Andreas Hirsch**

Keywords:
functionalization · graphene · graphene oxide · spectroscopy · synthetic methods

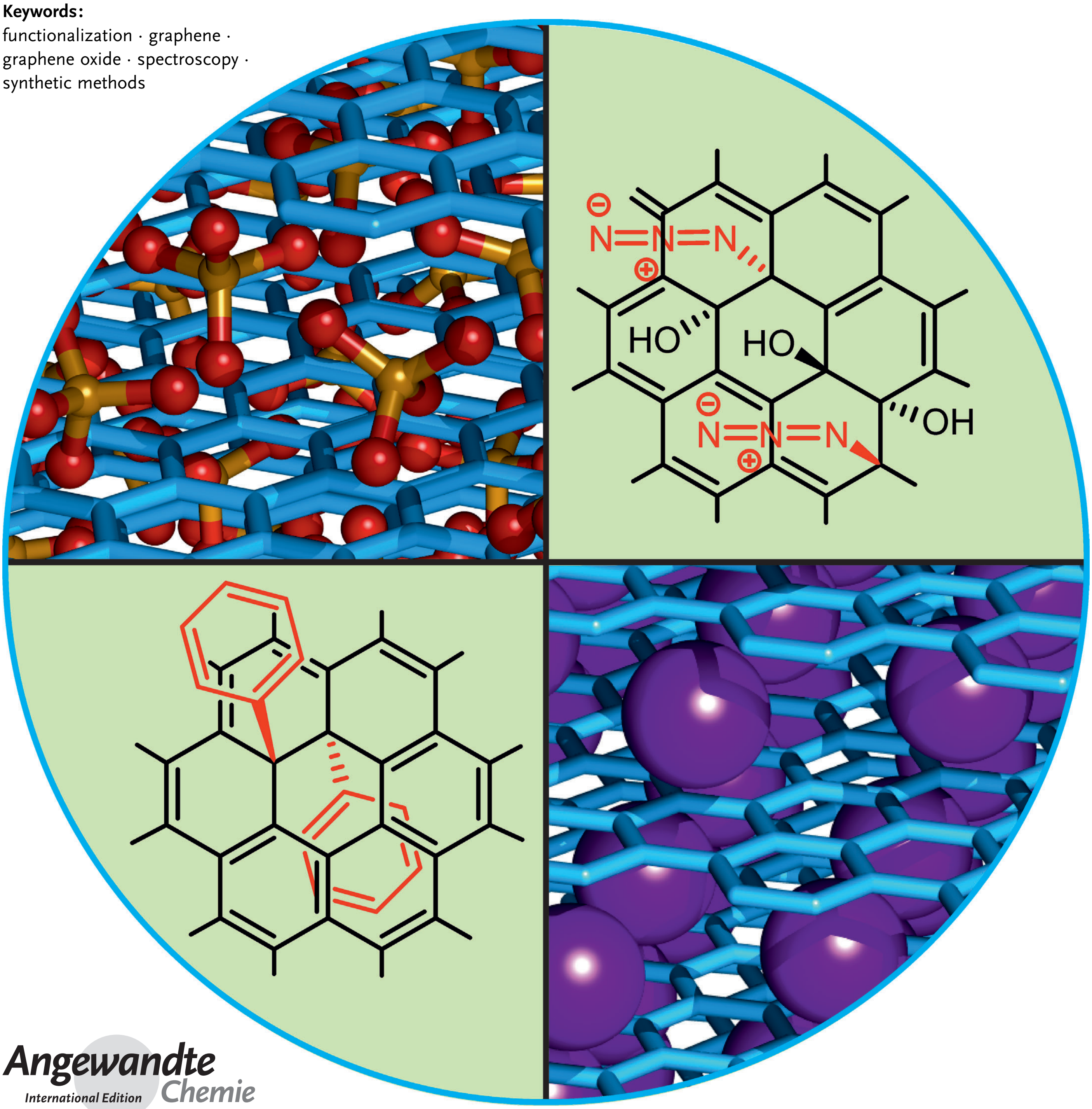

The chemical production of graphene as well as its controlled wet chemical modification is a challenge for synthetic chemists. Furthermore, the characterization of reaction products requires sophisticated analytical methods. In this Review we first describe the structure of graphene and graphene oxide and then outline the most important synthetic methods that are used for the production of these carbon-based nanomaterials. We summarize the state-of-the-art for their chemical functionalization by noncovalent and covalent approaches. We put special emphasis on the differentiation of the terms graphite, graphene, graphite oxide, and graphene oxide. An improved fundamental knowledge of the structure and the chemical properties of graphene and graphene oxide is an important prerequisite for the development of practical applications.

From the Contents

1. Introduction: Graphene and Graphene Oxide—Opportunities and Challenges for Synthetic Chemists

Research into graphene and graphene oxide (GO) represents an emerging field of interdisciplinary science that spans a variety of disciplines, including chemistry, physics, materials science, device fabrication, and nanotechnology.[1] At the same time, the field of graphene and GO has quite a long history.[1d–f,2] The current graphene boom started in 2004 when Geim, Novoselov et al. published the deposition and characterization of single sheets of graphite on solid supports.[1a] Their groundbreaking experiments on graphene were honored with the Nobel Prize in Physics in 2010.[1b,c,3] Exceptional electronic, optical, and mechanical properties were discovered in quick succession as a consequence of the experience gained from other carbon allotropes.[4] In particular, the high charge carrier mobilities, the electrical and thermal conductivity, combined with transparency and mechanical strength make graphene highly attractive for future high-tech applications.

The current status of graphene technology with respect to prototype applications has been extensively reviewed.[6] Many graphene-based devices outperform reference systems, for example in high-frequency transistors, foldable and stretchable electronic or photdetectors,[6b,7] capacitors,[8] transparent electrodes,[9] sensors,[10] H_2 generation,[11] pollution management,[12] energy applications,[13] biomedical applications,[7b,14] and in composite materials.[15]

What role can synthetic and in particular wet chemistry play in the field of graphene and GO technology, and can it push the field a significant step further ahead? The last 20 years have already witnessed the chemical functionalization of other synthetic carbon allotropes, such as fullerenes and carbon nanotubes. This has led to many important accomplishments, such as improvement of solubility and processibility, the combination of properties with other compound classes, and last but not least the discovery of unprecedented reactivity principles.[16] Numerous well-defined covalent and noncovalent derivatives of fullerenes and nanotubes have been synthesized and many of those show outstanding properties. Conceptually, it can be expected that the chemical behavior of graphene and GO resembles those of fullerenes and carbon nanotubes, especially in terms of addition reactions to the conjugated π system. But significant differences are also to be expected, in particular because, in contrast to fullerenes and carbon nanotubes, graphene is a flat and strain-free system whose plane can be attacked from both sides when dispersed in a solvent.

Graphene is a two-dimensional (2D) carbon allotrope which can be viewed as both a solid and a macromolecule with molecular weights of more than 10^6–10^7 g mol^{-1}. In natural graphite, the graphene layers stick together through very pronounced π-π stacking interactions. This noncovalent interlayer binding contributes significantly to the high thermodynamic stability of graphite. As a consequence, the wet chemistry of graphene is always concerned with overcoming these interactions. For example, a targeted exfoliation of graphite or the stabilization of solvent-dispersed graphene sheets always competes with reaggregation. It should be pointed out that a solid sample of graphene can only be stabilized on a support, such as a surface. A nonsupported graphene powder can not be expected to exist, since at least a partial restacking to graphite will take place! Another possibility of stabilizing individualized graphene is to "mask" the surface through chemical functionalization.[17] To date, it has not been demonstrated that a graphite crystal can be completely dispersed into individualized graphene sheets in

---

[*] Dr. S. Eigler, Prof. Dr. A. Hirsch
Friedrich-Alexander-Universität Erlangen-Nürnberg (FAU)
Department Chemie und Pharmazie
and
Institut für Neue Materialien und Prozesstechnik (ZMP)
Henkestrasse 42, 91054 Erlangen (Germany)
and
Dr.-Mack Strasse 81, 90762 Fürth (Germany)
E-mail: siegfried.eigler@fau.de
andreas.hirsch@fau.de

solvent. However, the dispersion of a certain fraction can be accomplished through the assistance, for example, of a surfactant. The transformation of graphene into a derivative such as GO, however, can allow efficient wet chemical dispersion.[18] Despite such inherent difficulties and limitations of the wet chemistry, the functionalization of graphene is a very challenging but promising approach. Many exciting hybrid systems involving covalently bound functional building blocks can be imagined. For example, combining the electrical conductivity of graphene with selective recognition sites of addends may enable in vivo monitoring of biomolecules. To reach such ambitious goals, it is necessary to prove the formation and stability of chemical bonds to attached addends beyond any doubt. Furthermore, it is inevitable that the degree of functionalization on graphene derivatives will be identified and any possible side reactions controlled. Within the process of the chemical synthesis of a new compound, the purification and the unambiguous structural characterization of the reaction product represent key endeavors. However, in the case of graphene chemistry, this is a very difficult objective because of the polydispersity, polyfunctionality, and in many cases unfavorable solubility of the prepared derivatives. Moreover, classical methods used by synthetic chemists for decades to isolate and characterize new molecules, such as chromatography, mass spectrometry, and NMR spectroscopy, cannot be applied. Therefore, in addition to the development of successful concepts for the wet chemical functionalization of graphene and GO, new analytical tools for a satisfactory structure characterization have to be elaborated and applied.

In this Review we provide an overview on the state-of-art of the wet chemistry of graphene and GO. We will first outline the inherent and important characteristics of their structural composition. Then we will discuss suitable preparation methods to make graphene and GO available as a starting material for chemical modifications. Finally, we present functionalization concepts and also discuss open challenges for the synthetic chemistry of carbon allotropes.

2. Structure Definitions and Chemistry Concepts

In the literature one can often find the terms graphite, graphene, graphite oxide, and graphene oxide used without much care and they are often interchanged, which can be misleading. For this reason, we want to clarify these terms first, before we start with the subsequent discussion of the wet chemistry of graphene and GO.

2.1. Graphite

Graphite can be of natural origin or synthetically generated.[19] The 3D stacking of the individual sp^2 layers can either lead to a hexagonal (AB) or rhombohedral (ABC) stacking, or the structure can be turbostratic with no regularities within the layer sequence.[20] Samples of natural graphite comprise several portions of these structures, which influence the reactivity.[19] The ideal structure of graphite is shown in Figure 1, but flakes of natural graphite usually bear macroscopic cracks and holes that can significantly affect the chemical reactivity.

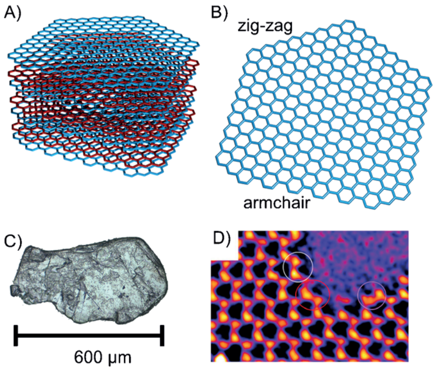

Figure 1. Schematic representation of A) the ideal structure of AB-stacked graphite and B) the structure of a sheet of graphene with zig-zag and armchair edges. C) Photograph of natural graphite with visible macroscopic cracks and holes. D) HRTEM image of graphene with one edge. Adapted from Ref. [5] with permission from Macmillan Publishers Ltd: Nature Communications, Copyright 2014.

2.2. Graphene

As depicted in Figure 1B graphene is a single layer of graphite and is built of sp^2-hybridized carbon atoms arranged in a honeycomb lattice. Here we use the expression G_1 as the

Siegfried Eigler received his PhD in organic chemistry from the Friedrich-Alexander-Universität Erlangen-Nürnberg in 2006 with Norbert Jux. He then worked on electrically conductive polymers at DIC Berlin and in 2008 he started his research on GO. In 2011 he became a lecturer at the Department of Chemistry and Pharmacy and a research associate at the Institute of Advanced Materials and Processes at the University of Erlangen-Nürnberg, and started his habilitation. His research focuses on the defect-free synthesis, structure evaluation, and controlled functionalization of GO.

Andreas Hirsch obtained his PhD in organic chemistry in 1990. After postdoctoral research at the Institute for Polymers and Organic Solids in Santa Barbara (USA), in 1991 he returned to Tübingen as a research associate at the Institute for Organic Chemistry. After his Habilitation in 1994, he joined the faculty of the Department of Chemistry at the University of Karlsruhe as a professor. Since 1995, he has been Full Professor of Organic Chemistry at the University of Erlangen-Nürnberg. His research focuses on synthetic carbon allotropes as well as supramolecular and nanochemistry.

descriptor for graphene. The subscript “1” denotes that exactly one layer of graphite is considered. Accordingly, two π-π-stacked graphite layers are denoted as G_2 and can also be called bilayer graphene. An aggregate consisting of less than ten layers ($G_{<10}$) is called few-layer graphene.

Although ideal graphene would be a plane of infinite dimensions, real graphene exhibits edges that have either a zig-zag or an armchair arrangement. The high-resolution transmission electron microscopy (HRTEM) image of graphene in Figure 1 D shows a graphene layer with a typical edge.[5] The atomic structure of edges becomes visible. Besides edge structures, lattice defects have also been studied by HRTEM.[21] The structure of graphene grown by chemical vapor deposition (CVD) on copper and subsequently transferred for analysis is shown in Figure 2.[21] In addition to some holes, merged graphene domains and so-called grain boundaries with broken hexagonal symmetry arising from five- and seven-membered carbon rings were found.[21,22] Structural defects can result in locally curved structures that cause local doping and, therefore, influence the reactivity of graphene.[23]

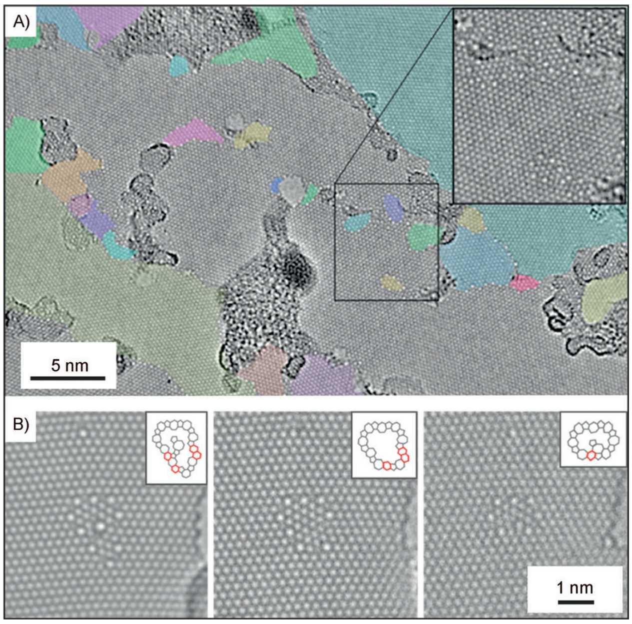

Figure 2. A) HRTEM image of graphene with grains marked in various colors; inset: magnification showing the grain boundaries; B) magnification of defect structures with five- and seven-membered carbon rings. Reproduced from Ref. [21] with permission from the American Chemical Society, Copyright 2012.

2.3. Graphite Oxide and Graphene Oxide

The properties and applications of GO have been extensively reviewed.[6a,24] GO is a single layer of graphite oxide. During the formation of graphite oxide, the graphene layers in graphite become intercalated by an acid to form a stage 1 intercalation compound, with all layers being intercalated. Subsequent oxygenation of such stage 1 intercalation compounds occurs on both sides of the basal plane and in this way graphite oxide is formed. Delamination of single layers of graphite oxide leads to GO (Figure 3). The exact nature of the functional groups in GO strongly depends on the reaction conditions, such as preparation time and temperature as well as on the work-up procedure. Typically, GO consists of about 45 mass% carbon. Although several structure models have been proposed, GO is a rather polydisperse material, whose exact structure is very difficult to precisely define.

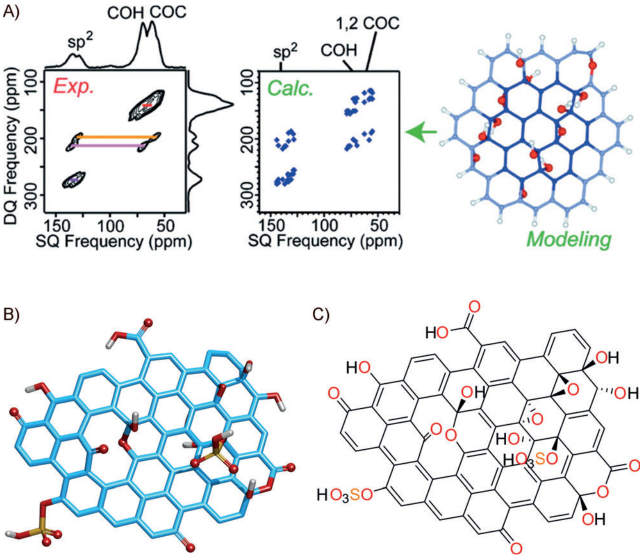

Figure 3. A) ^{13}C NMR spectroscopic investigation of ^{13}C-labeled graphite oxide; DQ = double quantum, SQ = single quantum. Reproduced from Ref. [25] with permission from the American Chemical Society, Copyright 2010. B) Structural model of GO with organosulfate groups in addition to hydroxy and epoxy groups on both sides of the basal plane and hydroxy, carbonyl, and lactol groups as well as carboxylic acids at the edges. A proposed defect hole structure stabilized by an adjacent carbonyl group and a hemiacetal arising from the loss of one carbon atom is shown.[26] C) structural formula of the structural model displayed in (B).

Furthermore, defects within the σ framework of the C skeleton can easily form upon overoxidation. This process is always accompanied by the release of CO_2. These defects in GO are difficult to characterize precisely and are impossible to heal without completely reassembling the carbon framework, which would require temperatures > 1500 °C.[27] As outlined in Section 3.2.3, the defect density can be estimated after chemical reduction.[28] We have recently invented a new synthesis procedure for GO that preserves the carbon framework to a very large extent, and only a minor number of σ hole defects are generated with a residual defect density as low as about 0.01%.[29] Therefore, this new type of GO exhibits an almost perfect honeycomb lattice. We denote this graphene oxide with an almost intact carbon framework ai-GO. The difference between graphene derived from conventionally prepared GO and ai-GO is illustrated in Figure 4.

2.3.1. “Oxo” Functionalities on Graphene and GO

The most suitable structure model for GO is based on the investigations of Lerf, Klinowski, and co-workers and was confirmed and advanced by the the research groups of Ishii and Gao.[25,26b,30] Along these lines, ^{13}C-labeled graphite oxide

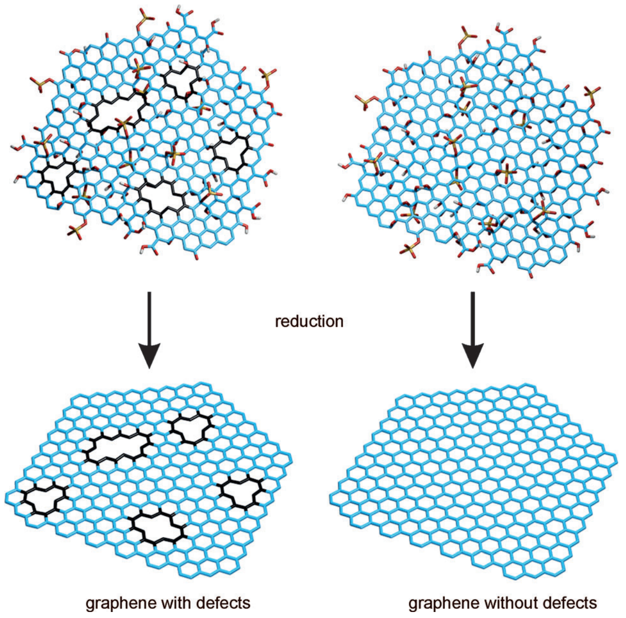

Figure 4. GO with σ-hole defects can only be converted into graphene with σ-hole defects; residual functional groups at the edges are omitted. On the other hand, ai-GO can be reduced to almost intact graphene.[27]

was also synthesized and analyzed by solid-state NMR spectroscopy.[25] The results strongly suggest that hydroxy and epoxy groups are in proximity to each other (Figure 3A) and a large portion of sp^2-hybridized carbon remains preserved during oxidation. If GO is synthesized in sulfuric acid, GO with a sulfur content of up to 6% can be found, with the sulfur content originating from covalently bound sulfate (Figure 3B).[26a] This organosulfate is hydrolytically stable in pure water under ambient conditions and can be distinguished from adsorbed inorganic sulfate. Furthermore, it contributes to the acidity of GO and enables chemical reactions.[31]

2.3.2. *Addends at Edges and Defect Sites*

NMR spectroscopy led to the identification of lactol groups at the edges of graphene, and are represented in the GO model of Figure 3.[26b] Other O functionalities are carboxylic acids as well as hydroxy and carbonyl groups. It should be kept in mind that the edges of graphene/graphite have either an armchair or a zig-zag arrangement. Edge oxidation leads to carbonyl or hydroxy groups. The formation of carboxy or lactol groups requires the breaking of C−C bonds, which may be accompanied by the loss of carbon induced by overoxidation and CO_2 formation during synthesis.

In general, by following the preparation procedures by Brodie,[32] Staudenmeier,[33] or Hummers and co-workers,[34] the loss of carbon and formation of CO_2 cannot be prevented. Recent results suggest that about one CO_2 molecule per 35–55 lattice carbon atoms is already formed during the oxidation process and the final product bears about one carbonyl group per 10–12 lattice carbon atoms.[35] The loss of carbon from the carbon framework consequently results in permanent defects, including holes of various sizes (Figure 4). Edges at defect sites are terminated by oxygen functionalities, as indicated by the proposed structures in Figure 3B,C.

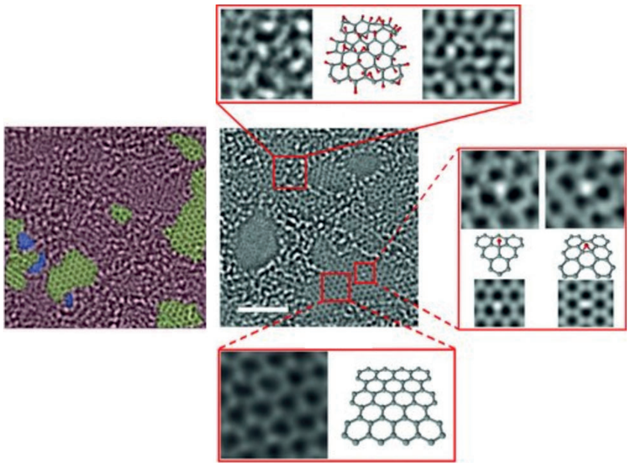

Figure 5. HRTEM image of GO displaying the preserved regions (green) of graphene (1–2 nm), holes (blue), and heavily oxidized regions (red); insets: comparison of the measured and simulated images with structural models. Reproduced from Ref. [36] with permission from Wiley-VCH Verlag GmbH & Co, Copyright 2010.

The heterogeneous structure of GO can be visualized by HRTEM imaging (Figure 5).[36] It comprises oxidized regions beneath small preserved aromatic regions. However, it remains difficult to visualize defects consisting only of single atoms.[36] Further insight was provided by STM investigations on GO.[37] These structural insights demonstrate that GO is not a defined material and it is important to keep in mind that the chemical composition, type, and amount of oxygen addends depends on the preparation procedure.

3. *Formation of Graphene and Graphene Oxide*

Graphene generation by wet chemical approaches has been accomplished by a variety of methods, each having advantages and limitations. Non-wet chemical methods, which provide access to small amounts of high-quality graphene on surfaces, are also outlined briefly for comparison.

3.1. *Non-Wet Chemical Methods for the Production of Graphene on Surfaces*

A typical non-wet chemical method for the production of graphene is based on chemical vapor deposition (CVD) on metal surfaces at about 1000 °C. A preferred surface for the synthesis is copper, which can be used to make continuous films of graphene. However, such films contain grain boundaries and the graphene needs to be transferred onto the desired surface.[38]

A few individual flakes of graphene can be obtained by mechanical cleavage using an adhesive tape.[1a] These flakes, if placed on a Si wafer with a 300 nm thick layer of SiO_2, are visible with an optical microscope, or even by the eye, which is beneficial for many investigations on single sheets of graphene.[1a,39] Moreover, graphene from SiC (epitaxial growth) can be obtained; however, isolation of graphene remains a complex procedure.[40] These methods are not suitable for chemical bulk functionalization. Nevertheless, since the chemical structure bears very low densities of defects (approximately 0.01–0.001 %), this graphene is suitable for the evaluation of reactions, since the reactions can be easily identified by Raman spectroscopy, as explained in Section 3.2.3.[41]

3.2. *Wet Chemical Synthesis of Graphene Oxide and Graphene*

The oxidation of graphite to graphite oxide, which is synonymously also termed “graphitic acid”, was first described by Schafhaeutl in 1840.[42] In 1855, Brodie discovered the formation of yellow graphitic acid after oxidizing graphite in nitric acid with potassium chlorate as the oxidant.[43] Staudenmaier optimized the procedure to minimize the risk of explosions caused by the accumulation of ClO_2.[33,44] In 1909, Charpy described the oxidation of graphite in sulfuric acid using potassium permanganate as the oxidant, keeping the temperature below 45 °C to suppress the extensive formation of CO_2.[45] The same procedure, which was shown to be scalable, was later called Hummers method.[34,46] Hummers procedure can be applied on a multigram scale in the laboratory and is the most frequently used method to prepare graphite oxide and its single layers, which are obtained after delamination in a suitable solvent. These single layers are called graphene oxide.

3.2.1. *Reaction Intermediates during the Oxidation of Graphite in Sulfuric Acid with Potassium Permanganate as Oxidant*

The oxidation mechanism of graphite in sulfuric acid is not fully understood. However, there is evidence for several key intermediates. In general, natural graphite is used as the starting material to enable the large-scale synthesis of GO (Figure 6). In the first step, graphite is dispersed in sulfuric acid, which becomes intercalated in the presence of an oxidant. This leads to the formation of graphite sulfate, a graphite intercalation compound (GIC).[47] The intercalation is accompanied by an increase in the layer distance, which results in activation of the graphite. It was assumed that either permanganate or in situ formed dimanganese heptoxide are the active oxidants.[24c] The oxidation species must be able to diffuse readily through the interlayer space of graphite sulfate. As a consequence, manganese esters are formed. It is desirable to control this process to prevent overoxidation, formation of CO_2, and the resulting impossible-to-heal hole defects in the graphene lattice. The hydrolysis of manganese esters and the solubilization of manganese–oxo species are accomplished by the addition of water and hydrogen peroxide. It is reasonable to assume that cyclic organosulfate groups are formed during the oxidation after partial hydrolysis of manganese esters in sulfuric acid.[35] The subsequent work-up procedure either favors the hydrolysis of cyclic organosulfate to organosulfate or complete hydrolysis, which may be promoted by the action of hydrochloric acid at elevated temperatures.[26a,48] Graphite oxide is purified by centrifugation and re-dispersion in water or by dialysis.[49] Delamination of graphite oxide to GO in water can be facilitated by sonication. GO can be dispersed in water and polar solvents and can be processed as single layers by various techniques, including the Langmuir–Blodgett method or by spin coating (Figure 6 B,C).[18,50] The size of deposited GO flakes typically varies between 10–100 nm and up to 100 μm.[51]

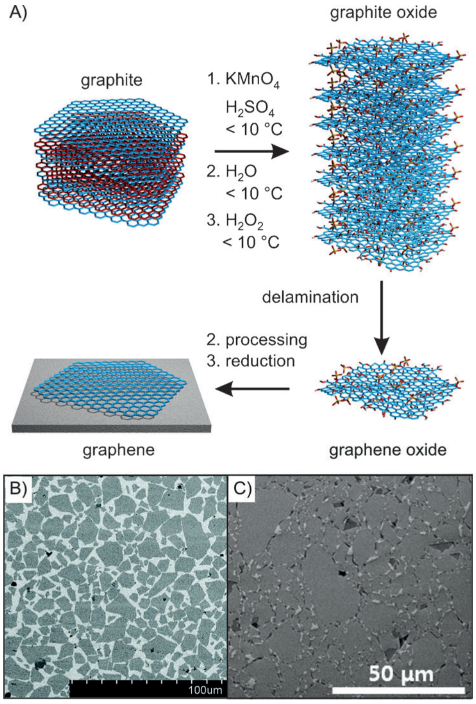

Figure 6. A) Synthesis of ai-GO and graphene, starting from graphite in sulfuric acid with potassium permanganate as the oxidant; SEM images of B) a Langmuir–Blodgett film of GO[50a,b] (reproduced from Ref. [50a] with permission from the American Chemical Society, Copyright 2009); and C) a spin-coated GO film (reproduced from Ref. [50c] with permission from the American Chemical Society, Copyright 2013).

Controlling the reaction temperature (< 5–10 °C) during both the oxidation step and especially the work-up prevents to a very large extent the overoxidation of graphene layers. This procedure enables the isolation of GO with an almost intact σ framework of C atoms (ai-GO) with a defect density as low as 0.01 %.[29,52]

3.2.2. *Reduction of GO to Graphene*

The reduction of GO to graphene has been approached by a variety of methods.[53] The most simple way is thermal annealing, which causes disproportionation of GO into CO_2 and graphene. Although this method is attractive due to its simplicity, perfect graphene is not obtained, even at temperatures up to 1100 °C. Instead, a ruptured carbon framework is obtained that contains σ-hole defects functionalized with oxygen functionalities, such as carbonyl groups or ethers (Figure 4).[54] Temperatures higher than 1500 °C are required for the complete deoxygenation of GO, which causes reorganization of the carbon framework.[27] Such conditions are not favorable due to the high energy cost or the incompatibility with temperature-sensitive substrates. Furthermore, CVD methods are superior for generating higher quality graphene at even lower temperatures. The only reversible addition and thermal removal of oxygen atoms to graphene was reported for low concentrations of oxygen atoms in a vacuum.[55] Under other conditions, the irreversible generation of defects within the σ framework of C atoms occurs. Attempts to repair defects within the carbon framework by using small organic molecules at > 800 °C was only partially successful.[56] Therefore, the use of reducing agents in combination with an annealing step up to 200 °C has been targeted. Typical reducing agents are hydrazine and hydriodic acid.[53c] The common feature of all the methods is that intact graphene cannot be obtained from defective GO.

Evaluation of the local graphene domains was possible by HRTEM after reduction of GO at 800 °C using hydrogen plasma (Figure 7). Despite these harsh and non-wet chemical reduction conditions, the intact graphene domains are not larger than 1–9 nm² at best.[57] When hydrazine was used as the reducing agent nitrogen was found to be incorporated into the carbon lattice as revealed by NMR spectroscopy.[58] Scanning tunneling microscopy (STM) imaging suggests that residual defects are often decorated with oxygen functionalities, such as carbonyl groups.[59]

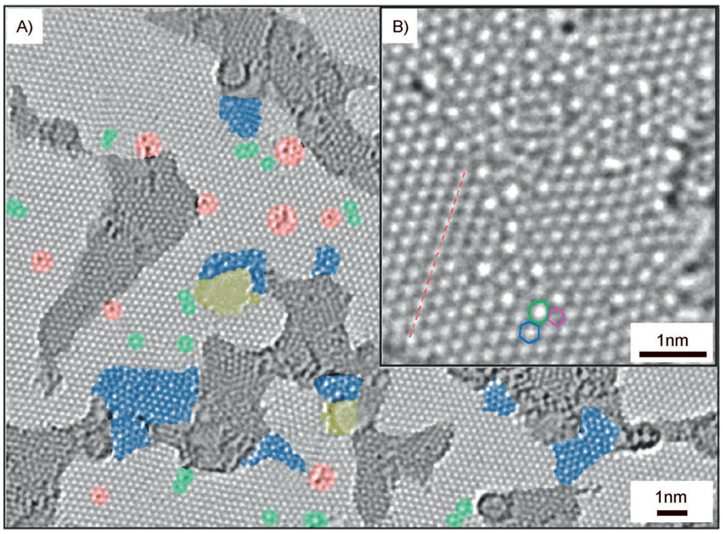

Figure 7. A) HRTEM image of reduced GO (reduced at 800 °C, H_2) displaying preserved regions of graphene (gray), contaminated regions (dark gray), disordered regions (blue), individual ad-atoms or substituted atoms beneath isolated topological defects (green), and holes (yellow). B) Magnification of a defect-rich region. Reproduced from Ref. [57] with permission from the American Chemical Society, Copyright 2010.

As indicated in Section 2.3, we have recently developed a method for the synthesis of ai-GO with an almost intact σ framework by preventing the evolution of CO_2 during synthesis by temperature control (< 5–10 °C) in the oxidation and aqueous work-up.[29] The reduction of ai-GO with HI indeed leads to the formation of graphene with a defect density of about 0.01 % (average distance of defects (L_D) up to 14 nm).[29] In this way, films of graphene flakes with an average defect density of 0.08 % could be produced.[52] The determination of L_D and the defect density can be accomplished by statistical Raman microscopy (SRM), a method that we introduced recently.[60] The efficiency of the applied reducing agents for ai-GO was studied and it was revealed that reduction with HI is more effective than that with hydrazine or thermal treatment.[52]

3.2.3. *Determination of the Defect Density and the Degree of Functionalization by Raman Spectroscopy*

Raman spectroscopy is one of the most powerful methods for characterizing graphene, GO, and their covalent derivatives.[61] The evaluation of the full-width at half-maximum (Γ) of peaks in Raman spectra can be correlated with the density of defects introduced by covalent functionalization.[62] Raman spectra of graphene display three major bands: the G band, the defect-activated D band, and the 2D band (Figure 8). When sp³ defects are introduced into the basal plane of graphene all the bands broaden and the I_D/I_G ratio increases to about 4:1 when a green laser is used for excitation (Figure 8 B, 9 A). At this maximum, L_D is about 3 nm and the defect density is about 0.3 %. For $L_D < 3$ nm, the I_D/I_G ratio decreases again and additional band broadening takes place (Figure 8 C). An idealized illustration of the degree of functionalization and defect density with $L_D = 10$ nm (0.03 %) is shown in Figure 8 C. Scanning films of graphene with a certain increment (micrometer scale) and recording several thousands of spatially resolved spectra is the basis of statistical Raman microscopy (SRM), a very powerful analysis tool that we established recently (Figure 9) for the visualization of the heterogeneity of the samples.[60]

In particular, Raman spectroscopy provides information about the integrity of the carbon framework. The intensity of the D band increases upon successive introduction of either holes or sp³ centers as a result of covalent binding of the addend. It is not possible, however, to distinguish between holes and sp³ defects by Raman spectroscopy.[28,60a] As a consequence, the D band signal can be used for both the determination of the quality of the graphene obtained by the reduction of GO,[28,52,60b] and for the degree of functionalization of graphene.[60a] This correlation holds for the case where the defect density is not higher than about 1 %.

3.2.4. *Approaches towards Generation of Graphene*

The most important methods for synthesizing graphene are summarized in Figure 10. Sheets of graphene prepared on a surface are mostly obtained by CVD methods,[38c,d,64] epitaxial growth,[65] mechanical cleavage,[39] or from ai-GO.[29] The wet chemical dispersion and exfoliation of graphite was expected to be a rather attractive method for the bulk production of graphene.[66] However, despite many

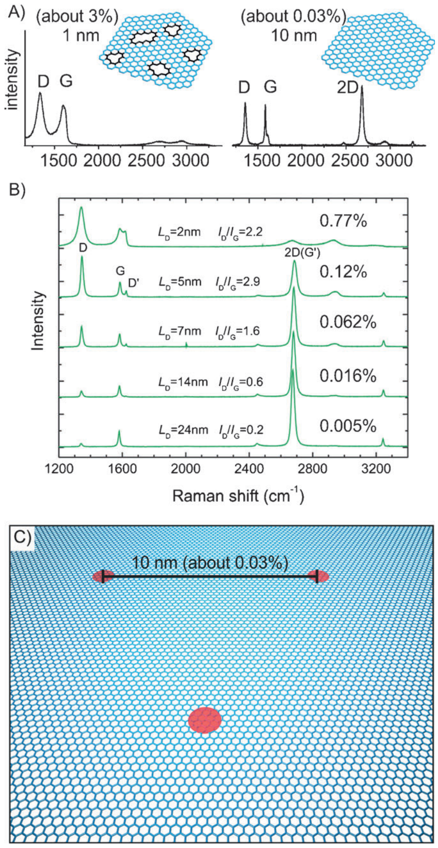

Figure 8. A) Raman spectra of graphene; left: GO with a defect density of 1–3 % and right: ai-GO with 0.03 % defects; insets: simplified structural models of graphene with defects and without defects. B) Raman spectra of graphene with L_D values between 2 and 24 nm (defect densities given in %). Reproduced from Ref. [62a] with permission from the American Chemical Society, Copyright 2011. C) Illustration of an idealized distance pattern of defects of 10 nm.

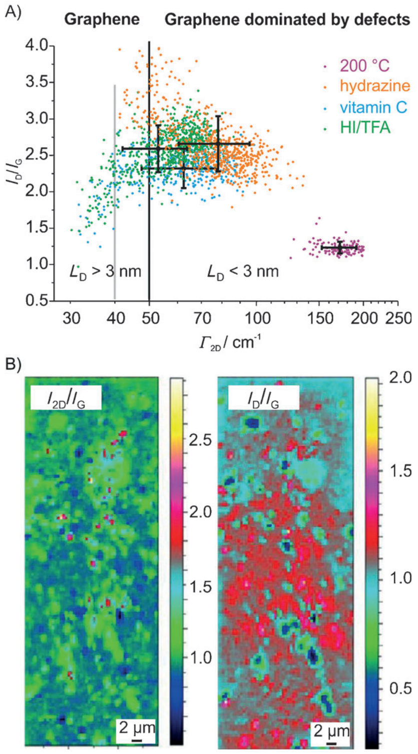

Figure 9. A) Illustration of statistical Raman microscopy analysis of films of ai-GO by plotting I_D/I_G versus Γ_{2D}: reduced by thermal treatment, hydrazine, vitamin C, or HI/TFA. Reproduced from Ref. [52] with permission from The Royal Society of Chemistry. B) SRM images of functionalized graphene from the reaction of C_8K and 4-*tert*-butylphenyldiazonium tetrafluoroborate displaying local variations in films (I_{2D}/I_G and I_D/I_G). Adapted from Ref. [63] with permission from Macmillan Publishers Ltd: Nature Chemistry, Copyright (2011).

approaches using surfactants, for example, sodium cholate (Figures 10 B and 11) in water, or solvents with high boiling points, such as *N*-methylpyrrolidone, it remains challenging to reach a quantitative stabilization of individual graphene sheets.[67] Furthermore, species adsorbed on graphene, including solvents with high boiling points, are difficult to remove.[68]

These exfoliation approaches result in few-layer graphene with a flake diameter of about 150 nm on average being formed in quite large portions. This outcome is also due to the fact that graphite tends to break apart when exposed to mechanical treatment such as ball milling or sonication.[68b,69] Density gradient ultracentrifugation was used to analyze the number of graphene layers of sonicated samples (Figure 11). Besides flakes of few-layer graphene, a certain fraction of real single-layer graphene with a somewhat increased density of defects was identified.[70]

In donor-GICs (graphite intercalation compounds) the negatively charged graphene layers, called graphenides, are separated from each other, for example, by potassium or lithium ions.[47a,b,d,71] However, wet chemical delamination to single layers of graphenide was demonstrated only for flakes with a diameter of about 150 nm.[72] The number of layers can, for example, be counted by the number of fringes in the HRTEM images.[73]

Acceptor-GICs, such as graphite sulfate, can be prepared on a technical scale and exfoliation can be achieved by inducing thermal decomposition of the intercalated species.[74] Few-layer graphene that partially reaggregates in the solid state are generally obtained by this method.[75] Furthermore, graphene and few-layer graphene can be generated through dispersion directly from an acceptor-GIC by using oleyl amine, for example, for stabilization.[76]

GO can be reduced to graphite in solids or in solution, and without a stabilizer solids are formed due to aggregation (Figure 10 D).[77] Here, the defect density depends on the preparation conditions and additional defects are clearly formed during thermal reduction due to carbon loss. GO can also be reduced in dispersions in the presence of a surfactant to form stabilized graphene.[77b] However, surfactants generally remain strongly adsorbed, although the sodium salt of binol was reported to be removable.[78]

Recently, an efficient electrochemical exfoliation method of graphite was demonstrated by using diluted sulfuric acid as a reactive solvent. This approach yielded graphene, predominantly bilayer graphene, and few-layer graphene, and the

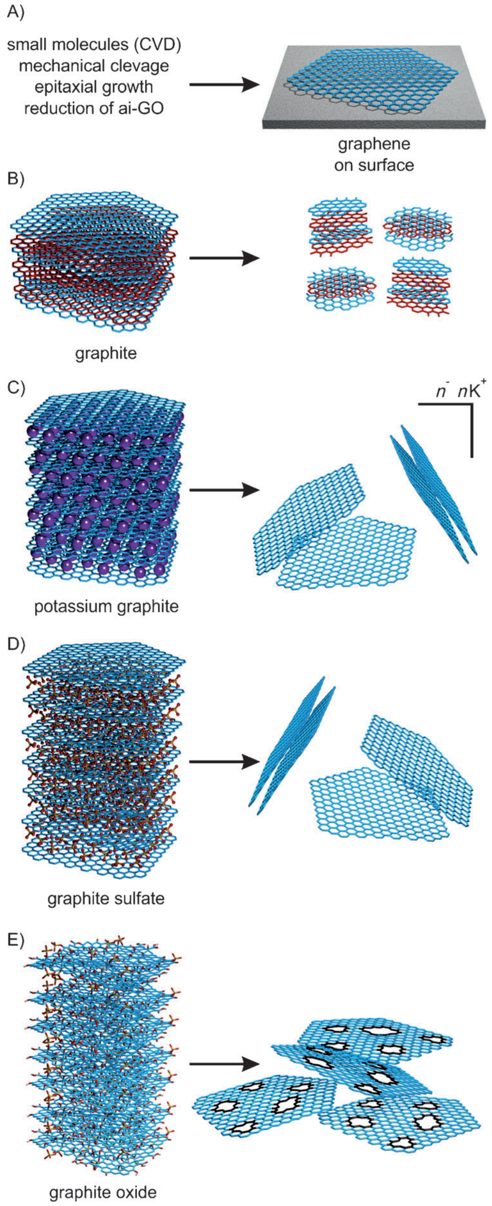

Figure 10. Synthetic approaches towards graphene and few-layer graphene: A) from small molecules by CVD, mechanical cleavage, epitaxial growth, or from ai-GO; B) from graphite by sonication in solvents or ball milling, possibly with the aid of surfactants; C) from donor-GICs, such as C_8K in inert solvents; D) from acceptor-GICs by thermal treatment or liquid exfoliation; E) from graphite oxide by thermal treatment.

defect density of bilayer graphene could be estimated to be about 0.009 %.[79]

Reliable investigations on the functionalization of graphene require graphene with a defect density below 0.5 %, and graphene derived from ai-GO, for example, fulfills this demand.[29,52] At a higher defect density, changes in the degree of functionalization cannot be detected by Raman spectroscopy, which is the method of choice for the characterization of functionalized samples.

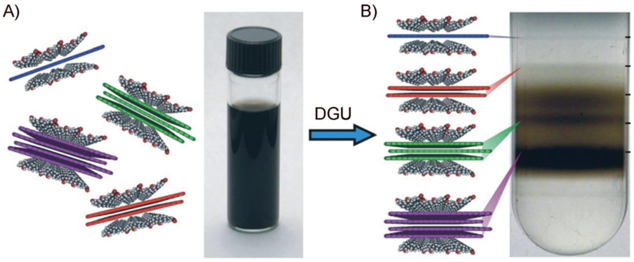

Figure 11. A) Polydisperse dispersion of graphene and few-layer graphene stabilized with sodium cholate as a surfactant. B) Fractions of graphene, bilayer, and few-layer graphene after density gradient ultracentrifugation (DGU). Reproduced from Ref. [70] with permission from the American Chemical Society, Copyright 2010.

4. Noncovalent and Covalent Modification of Graphene

The functionalization of graphene and few-layer graphene has recently been summarized in some specialized reviews.[6a,80] Here, we show examples that clearly relate to the functionalization and isolation of functionalized single layers of graphene (G_1). Methods that lead to functionalized few-layer graphene ($G_{<10}$) or graphite are only briefly mentioned.

In general, noncovalent chemistry is attractive because of the preservation of the conjugated π system. The noncovalent functionalization is based on weak interactions between graphene and a binding partner such as a surfactant, which can also be considered to be a ligand. Graphene derived from GO was also combined with surfactants for stabilization.[81]

For the covalent functionalization of graphene, a covalent bond must be formed, which is accompanied by the rehybridization of C atoms from sp^2 to sp^3. Although C–O bonds are formed during the synthesis of GO, C–C bonds can be formed through the use of diazonium compounds, which will be highlighted in Section 4.2.1.

4.1. Noncovalent Approaches

As depicted in Figure 11, the interaction of graphite with surface-active molecules (surfactants), such as sodium cholate,[70a,82] cetyltrimethylammonium bromide,[83] polyvinylpyrolidone,[84] triphenylene,[85] or pyrene derivatives,[86] is reported to produce noncovalently functionalized graphene. However, one has to keep in mind that, in addition to single-layer graphene G_1, large portions of few-layer graphene and even dispersed graphite are also obtained by this approach.

Coronene carboxylate has also been used as a surfactant, which allowed the generation of small flakes with diameters of a few 100 nm.[87] These graphene samples exhibit a defect density in the range of 0.03 %. Larger flakes of graphene G_1 together with few-layer graphene were obtained using a water-soluble perylene, as determined from the Γ_{2D} value in the Raman spectra (Figure 12).[17,88] The water-soluble perylene can delaminate and stabilize graphene with a flake size of about 1 µm and a moderate defect density of

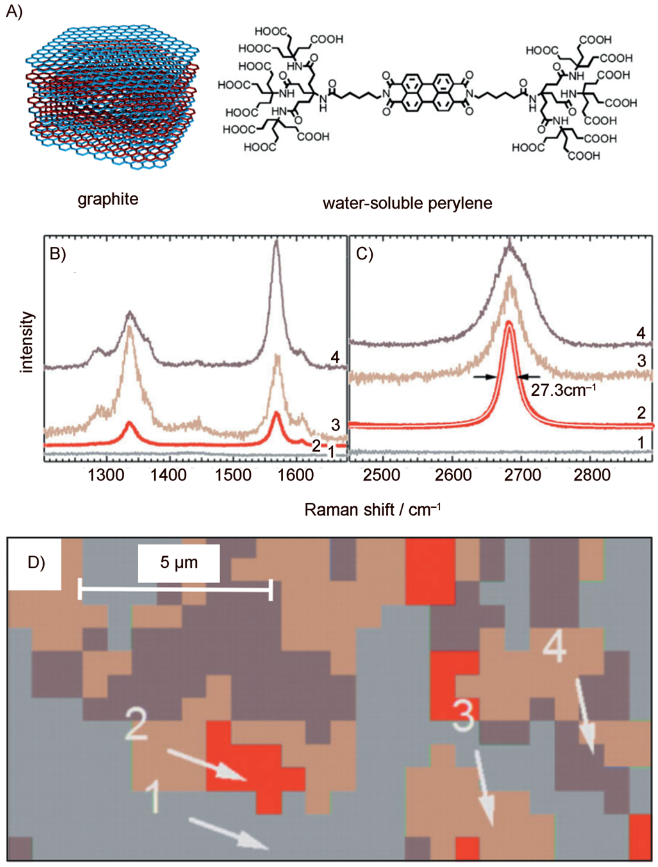

Figure 12. A) A water-soluble perylene which is able to exfoliate graphite. B) Raman spectra of delaminated graphene from positions 1–4 (in (D)), showing the D and G bands, position 2 relates to graphene (G_1). C) Raman spectra showing the 2D bands; $\Gamma_{2D} < 30\ \text{cm}^{-1}$ relates to graphene. D) Raman microscopy image color-coded according to the Γ_{2D} value; substrate (1), graphene (2, $\Gamma_{2D} = 25$–$39\ \text{cm}^{-1}$), few-layer (3, $\Gamma_{2D} = 39$–$65\ \text{cm}^{-1}$), and other areas (4, $\Gamma_{2D} > 65\ \text{cm}^{-1}$). Reproduced from Ref. [17] with permission from Wiley-VCH Verlag GmbH & Co, Copyright 2009.

approximately 0.01 %, as indicated by the D band (Figure 12).[17] The presence of defects may be a prerequisite for the successful delamination. The line shape of the 2D band clearly indicates the presence of single-layer graphene, since $\Gamma_{2D} < 39\ \text{cm}^{-1}$. The SRM image (Figure 12 D) also reveals the polydisperse nature of the sample.

4.2. Covalent Approaches

The covalent functionalization of graphene, few-layer graphene, and graphite is a growing field of research and is summarized in several reviews.[80,90] In principle, wet chemical functionalization allows for covalent binding to both sides of the graphene plane, which has a theoretical surface area of $2630\ \text{m}^2\,\text{g}^{-1}$. However, as illustrated, for example, in Figure 13, no exhaustive wet chemical functionalization of graphene with large organic molecules, such as phenyl groups, is possible for steric reasons, at least when the addends are only bound on one side of the basal plane. Even the complete hydrogenation of graphene, which leads to graphane with only sp^3-hybridized C atoms, has not yet been realized.[91] The highest degree of functionalization, which approaches the 1:1 stoichiometry, was achieved by the reaction of graphene with xenon difluoride to form fluorinated “graphane”.[92]

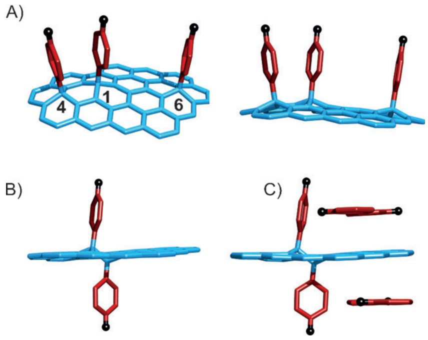

Figure 13. A) Graphene (blue) functionalized only on the upper side, e.g. with aryl moieties (red, black); 1,4- or 1,6-addition patterns are energetically favored, and the side view shows out-of-plane localization of the corresponding sp^3-hybridized C atoms.[89] B) Side view of graphene functionalized in the 1,2-position on both sides of the basal plane. C) An additional noncovalent binding of an aryl moiety by π-π stacking interactions is shown for comparison.

The chemical functionalization of graphene and few-layer graphene in dispersions was investigated using various reactants, including hydrogen, oxygen, or halogens, which led to partially functionalized graphene.[91–93] In the following, we describe the results of the wet chemical functionalization of graphene on a solid support and the wet chemical functionalization of graphene in dispersion.

4.2.1. Functionalization of Graphene on a Solid Support

In a first series of studies, graphene supported on SiO_2 was treated with electrophiles to study their reactivity toward graphene.[95] Theoretical calculations suggest that addends favorably add in the *cis*-1,4- or *cis*-1,6-positions if only one side of the graphene is accessible to reactants (Figure 13).[89] In contrast, addends react most likely in the *trans*-1,2-position if both sides of the graphene are accessible. In addition to the covalent binding, a competing noncovalent adsorption of reactants also has to be considered when reaction products are characterized.

A comparatively intensively investigated reaction type is the reaction of aryl diazonium compounds with graphene.[41,96] Figure 14 presents SRM images obtained after the treatment of graphene supported on SiO_2 with 4-nitrobenzenediazonium tetrafluoroborate. The reaction most likely involves an electron transfer from graphene to the diazonium ion followed by extrusion of N_2 and a subsequent addition of the aryl radical to the oxidized graphene layer. However, further investigations are required to understand all the details of the conversion. SRM allows the degree of functionalization of edges, central parts, and bilayer graphene to be visualized through analysis of the D band intensity or Γ_{2D} value.[94,97] The analyses reveal that edges of graphene are more reactive than the interior parts of the basal plane

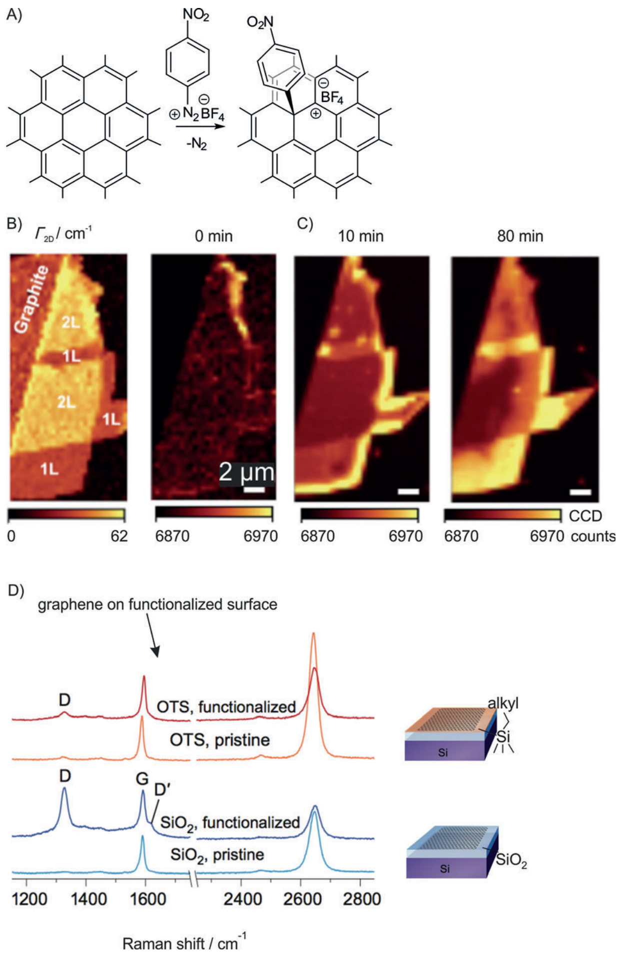

Figure 14. A) Reaction of graphene with a diazonium salt. B) Raman micropscopy image of mechanically cleaved graphene; left: mapping of Γ_{2D}; right: D band intensity. C) Mapping of the D band intensity after exposure of graphene to 4-nitrobenzenediazonium tetrafluoroborate after 10 and 80 min; Reproduced from Ref. [94] with permission from Wiley-VCH Verlag GmbH & Co, Copyright 2010. D) Raman spectra of graphene supported on different surfaces before and after functionalization with 4-nitrobenzenediazonium tetrafluoroborate. Adapted from Ref. [41] with permission from Macmillan Publishers Ltd: Nature Chemistry, Copyright (2012).

and that graphene is more reactive than bilayer graphene. The reason for the higher reactivity of graphene may be due to the corrugation of the graphene surface, which is more pronounced for single layers than for bilayers of graphene. Furthermore, adsorbed diazonium species could also be identified in this study, as illustrated in Figure 13C.

In another approach, graphene was deposited on either SiO_2 or on an alkyl-functionalized SiO_2 surface Figure 14D.[41] After the reaction of the diazonium compound, the Raman spectra reveal the distinctly higher reactivity of graphene on SiO_2 than on the alkyl-terminated surface. These approaches demonstrate that neutral graphene is not highly reactive towards diazonium compounds, but that an additional activation can facilitate the conversion.

It is interesting to note that a I_D/I_G ratio of 1:1 (Figure 14D) indicates a degree of functionalization of about 0.01%, and consequently the very small D band measured after the functionalization of graphene on the alkylated surface indicates that almost no reaction occurred. Thus, activation of graphene can enhance its reactivity, as was also demonstrated for graphene placed on nanoparticles, whereby graphene becomes locally curved.[98]

The wet chemical functionalization of graphene supported on SiO_2 was also carried out in a two-step process using reduced graphene (graphenide) as the starting material. Graphenide has the conceptual advantage that no oxidized graphene layers have to be generated (see also Figure 14) and at the same time graphenides are better reducing agents than neutral graphene itself. First, the supported graphene was reduced by treatment with a sodium/potassium alloy in dimethoxyethane (DME).[60a] The resulting surface-supported graphenide was then treated with phenyl iodide. In this case, an electron transfer from graphenide to phenyl iodide takes place to form iodide and phenyl radicals. The latter add to graphene (Figure 15). Other reactions, for example, photoinduced reactions of graphene with benzoyl peroxide, were also reported.[99]

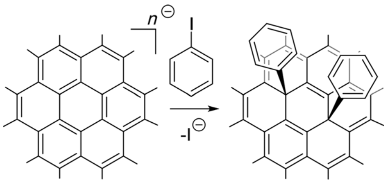

Figure 15. Wet chemical reaction of graphenide (activated graphene on a solid support) with phenyl iodide to form phenyl-functionalized graphene.[60a]

4.2.2. *Wet Chemical Functionalization of Graphene in Homogeneous Dispersion*

Since it has so far not been possible to generate a dispersion of completely exfoliated single-layer graphene, chemical reactions are carried out in mixtures, including few-layer graphene and dispersed graphite with diameters below 1 µm as predominant species. General approaches for the functionalization have been summarized in the literature.[90d,100]

Typical types of reactions are illustrated in Figure 16, such as hydrogenation,[93c,d,i] addition of phenyl radicals,[101] addition of diazonium species, or combined with [3+2] cycloaddition reactions to form 1,2,3-triazoles.[102] Furthermore, the addition of azomethine ylides,[103] fluorinated phenylnitrene species,[90e] aryne species generated from aryl trimethylsilyl triflates,[104] carbenes,[105] and Diels–Alder reactions with, for example, tetracyanoethylene were reported.[106] Moreover, acylation reactions were demonstrated to proceed at edges of few-layer graphene.[107] These types of reactions were also applied to introduce functional molecules on graphene so as to generate new properties, for example, the formation of dispersions,[90e,104] band-gap tuning for light harvesting,[100,108] and hydrogen storage.[109] Nevertheless, functionalized graphene has not been used in a systematic way for specific applications. Often, either the single-layer nature of function-

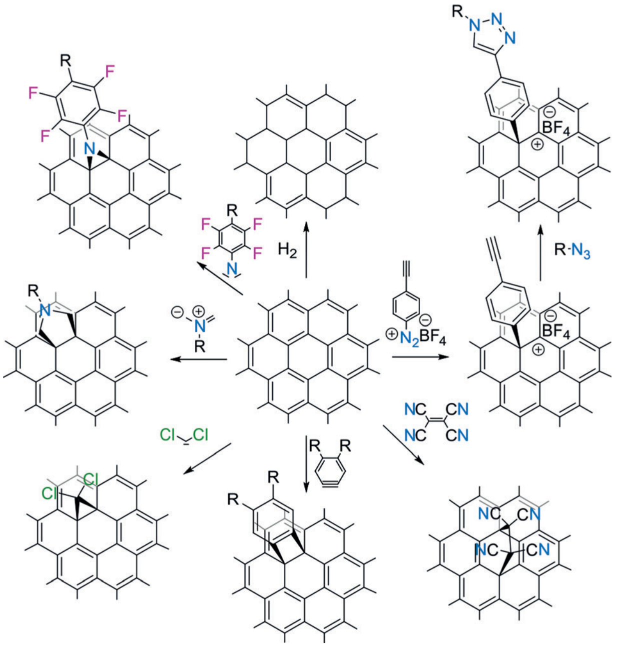

Figure 16. Selected reaction types for the functionalization of graphene and few-layer graphene.

alized materials is not proven or few-layer graphene is functionalized, which leads to covalently functionalized few-layer graphene that can be isolated in stacks (Figure 17 A). To overcome this obstacle for the functionalization of graphene, the activation of graphite prior to exfoliation provides an opportunity to address single layers so as to really synthesize functionalized G_1 graphene, even if stacks of functionalized G_1 graphene (G_1-R_n) are isolated (Figure 17 B).

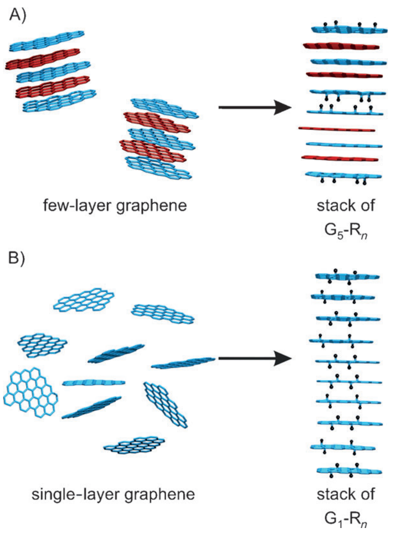

Figure 17. Schematic illustrations of the functionalization of A) few-layer graphene, as illustrated with five-layer graphene (G_5), which can be generated by dispersing graphite in solvents, and the isolated product G_5-R_n functionalized with *n* R groups. B) G_1 obtained, for example, by dispersing alkali-metal GICs and its subsequent functionalization to give, after work-up, stacks of functionalized G_1-R_n.

We have recently introduced a very suitable functionalization method for graphene, where negatively charged graphenides were used as activated intermediates for functionalization in homogeneous dispersions. Graphenides are present in donor-GICs, where for example alkali metals serve both as electron donors and intercalaters.[47a,b,d] Stable examples are C_6Li and C_8K, which represent activated reduced graphite. Furthermore, C_2Li is known but can only be formed under high pressure.[110] If donor-GICs are dispersed in a solvent such as DME, subsequent addition reactions with electrophiles can be carried out.[111]

An example is the reaction of graphenide with 4-*tert*-butylphenyldiazonium tetrafluoroborate in DME, which leads to the formation of arylated graphene G_1-aryl$_n$.[63] A similar reaction with *n*-hexyl iodide was also demonstrated (Figure 18).[112] Raman spectroscopic analysis of a flake of hexylated graphene reveals clear evidence for the single-layer nature of functionalized graphene and displays Γ_{2D} values $< 40\ \mathrm{cm}^{-1}$ and I_D/I_G values of about 2:1 (compare Figure 8 B). In this example, as shown by SRM, the degree of functionalization even varies within one flake of graphene.

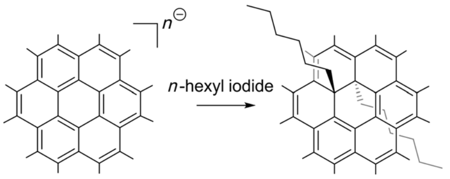

Figure 18. Conversion of graphenide into hexyl-functionalized graphene G_1-hexyl$_n$.[112]

Although the analytical methods for product characterization have improved recently, a detailed structural analysis of covalently functionalized graphene remains challenging. For example, it is still not straightforward to distinguish quantitatively between adsorbed and chemically bound species, which is a crucial prerequisite to reveal structure–property relationships.[63,113]

5. Functionalization of Graphene Oxide

GO is produced under harsh oxidative conditions and contains oxygen-based addends on both sides of the basal plane, as outlined in Section 3.2.1. However, synthetic procedures and work-up conditions strongly influence the composition of the functional groups.

5.1. Degradation of Graphene Oxide

The binding of functional groups on GO was found to be metastable even at room temperature,[114] and the thermally induced formation of CO_2 can be detected starting at 50 °C.[115] In addition, ^{18}O from adsorbed $^{18}OH_2$ is incorporated in the cleaved CO_2, which is very likely due to the formation of hydrates from carbonyl groups of GO.[115]

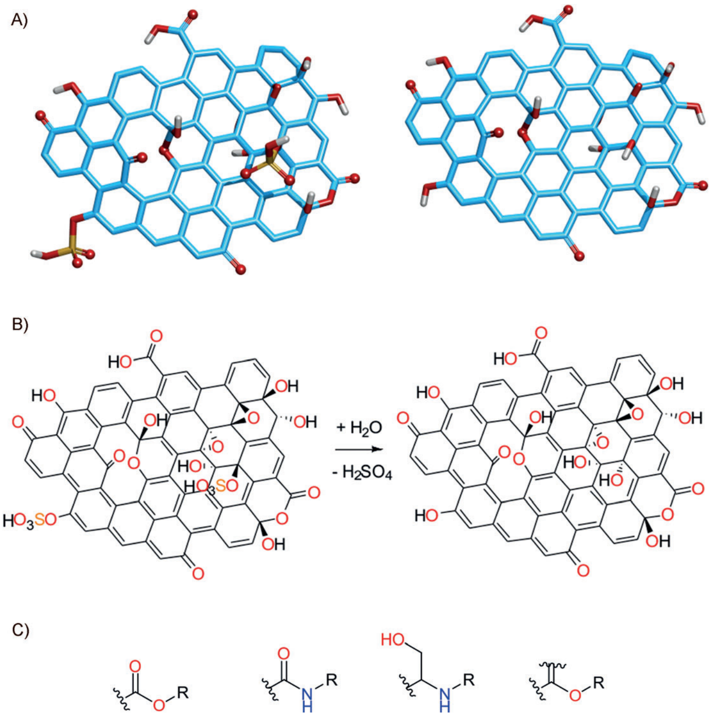

Figure 19. A) GO with different functionalities at the basal plane; left: with hydroxy, epoxy, and organosulfate groups, right: with hydroxy and epoxy groups. B) Illustration of the functional groups with a proposed structural defect as well as the hydrolytical cleavage of organosulfate. C) Typical chemical bonds formed during functionalization of GO.

Furthermore, degradation of GO can be used to partially explain the acidity of GO in water.[116] A large number of holes was found in steamed GO and these lead to porous materials.[117] Moreover, porous graphene was obtained after activating GO with potassium hydroxide before thermal exfoliation.[118] Finally, after prolonged degradation, GO turns into a material that is related to humic acid, as already described by Staudenmaier in 1899 (Figure 19).[44]

5.2. Transformation of Functional Groups in Oxo-Functionalized Graphene

5.2.1. Addressing the Surface of GO

When parts of the surface of GO are inaccessible to reactants because of coverage with attached substrates, the degree of GO functionalization is limited. Thus, the full potential and efficiency of a reaction is not tapped. Since both sides of GO are highly functionalized, complete delamination has to be achieved to allow for efficient chemical reactions. Density gradient ultracentrifugation studies used to separate GO sheets by size also revealed that some few-layered GO remains present in a minor amount even after sonication.[51b] Furthermore, concentration-dependent titrations of GO dispersions with methylene blue reveal that the maximum surface area of GO in water is accessible only at concentrations below 35 $\mu g\,mL^{-1}$ (Figure 20).[119] These experiments suggest that the delamination efficiency should be taken into account for the interpretation of analytical data.

5.2.2. Approaches for the Functionalization of GO

Carbonyl or carboxy groups formed during oxidative graphite degradation can be used for functionalization reactions.[120] In most approaches, carboxy groups are transformed to active esters and subsequently used for conversion into esters or amides (Figure 19 C).[121] Furthermore, the direct reaction of amines with graphite oxide and GO was also performed, which led to partially reduced and functionalized material.[122] The results are summarized in recent reviews.[10a,123]

Furthermore, several highly porous networks were prepared based on GO or their reduced forms, including the formation of aerogels.[124] One example that utilizes the hydroxy groups of GO is the cross-linking of GO sheets with benzene-1,4-diboronic acid to form boronic esters, thereby giving a 3D porous network attractive for gas adsorption (Figure 21).[125] Furthermore, organic isocyanates were used for functionalization.[126]

Determination of the amount of different functional groups and the evaluation of the efficiency of chemical reactions are still difficult tasks because of the amorphous and heterogeneous structure of GO. Reaction procedures well-known from organic chemistry can be applied to GO, and the successful reaction is often evaluated, for example, by the dispersibility or the performance of the materials in applications.

Nevertheless, GO and its derivatives have been used for various applications. Graphene derived from GO was used in transparent electrodes to make touch screens.[127] It was also found that GO can act as a surfactant to disperse carbon nanotubes.[128] Nano-GO with lateral dimensions < 50 nm was bound to polyethyleneglycol through an amine for drug delivery[120] and chemo-photothermal therapy.[129] Dye-labeled single-strand DNA was noncovalently bound to GO and the fluorescence was found to be quenched due to the interaction of the π systems.

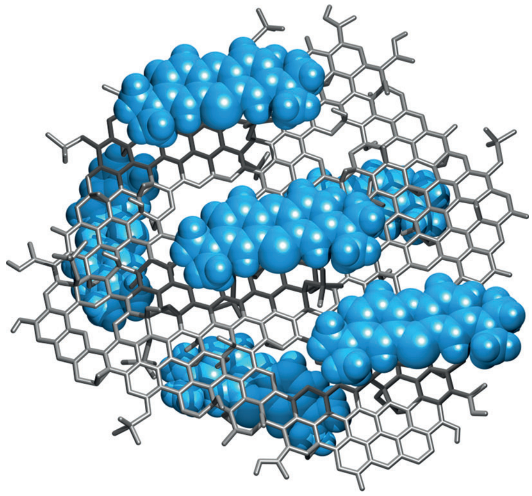

Figure 20. A) Illustration of GO (gray) with adsorbed methylene blue (blue) for the determination of the accessible surface area; the maximum surface area of GO is accessible at $c(\mathrm{GO}) < 35\ \mu g\,mL^{-1}$.[119]

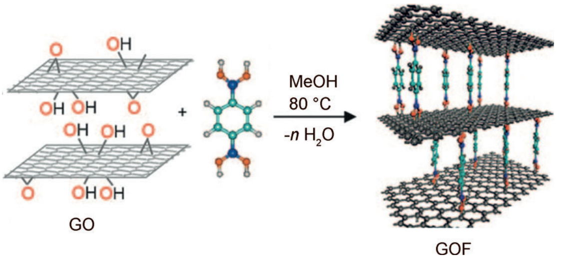

Figure 21. Reaction of hydroxy groups in GO with benzene-1,4-diboronic acid to form a stable porous framework. Reproduced from Ref. [125] with permission from Wiley-VCH Verlag GmbH & Co, Copyright 2010.

Adding a complementary target in nanomolar concentrations restored the fluorescence, and this concept was used to detect biomolecules.[130] GO was also used in sensors, for example, to detect humidity with a response speed of only about 30 ms.[131] In addition, GO functionalized by organosulfate and Cs^+ ions were used as hole- and electron-extraction materials, respectively, in polymer solar cells.[132] Composite materials of GO with small organic molecules or inorganic nanoparticles have been described, including for the preparation of supercapacitors.[6d] For example, stearylamine was used for the functionalization of GO to make composite materials with styrene.[133] Moreover, GO and its reduced form were used to make polymer composites by applying modern polymerization techniques.[15,77b,134] GO was also found to be a competitive material for charge storage.[135] This list of the functionalization approaches and applications is far from being complete. However, a much more detailed understanding of GO-based chemical reactions is desired to optimize functionalization concepts, because it is still challenging to determine the local structure of composite materials. Furthermore, it remains difficult to distinguish between functionalization at defect sides, of epoxy groups, or others.

5.2.3. *Functionalization of GO at the Basal Plane*

One approach to more controlled reactions started with the synthesis of ai-GO, which bears an almost intact σ framework of C atoms.[29] The carbon framework of ai-GO was found to be stable up to 100 °C, even if the functional groups started to cleave or transform.[136] Furthermore, proof was given that chemical reactions, such as the nucleophilic reaction of hydroxide with ai-GO, can be applied without degrading the carbon framework, provided the temperature is kept below 10 °C (Figure 22 A).[48] In particular, sodium azide was used to substitute organosulfate in ai-GO and to introduce a functional group that is suitable, for example, for use in subsequent azide–alkyne cycloaddition reactions (Figure 22 B).[31] The degree of functionalization, which can be up to one azide group per 30 C atoms, was determined by the amount of the sulfate leaving group. Furthermore, ^{15}N NMR spectroscopic studies using labeled azide reveal the absence of adsorbed azide, thus proving that covalent bonds have been formed exclusively.

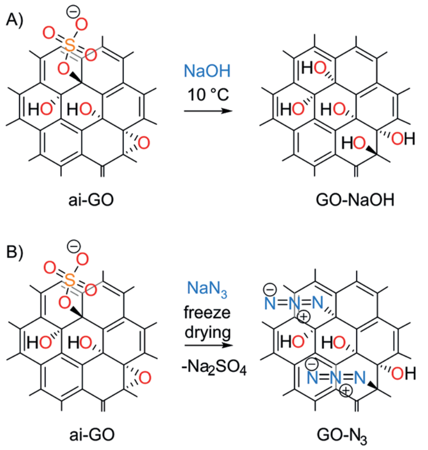

Figure 22. A) Reaction of ai-GO with hydroxide without further harming the carbon framework of ai-GO, a prerequisite for controlled chemical reactions with GO. Reproduced from Ref. [48] with permission from The Royal Society of Chemistry. B) Nucleophilic substitution of organosulfate groups of ai-GO by azide ions. Reproduced from Ref. [31] with permission from The Royal Society of Chemistry.

5.2.4. *Functionalization of Reduced GO*

As pointed out in Section 3.2, the reduction of normal non-ai-GO with a high defect density of approximately 1–3 % leads to graphene (also denoted as reduced GO) bearing a substantial number of σ defects, including holes, in the basal plane (see also Figures 4 and 10). Reduced GO was obtained by reducing GO in water with hydrazine hydrate and used for functionalization reactions, as illustrated by the selection of reactions in Figure 23. Reduced GO readily reacts with phenyldiazonium derivatives to provide functional molecules after further derivatization.[108,137] For the development of

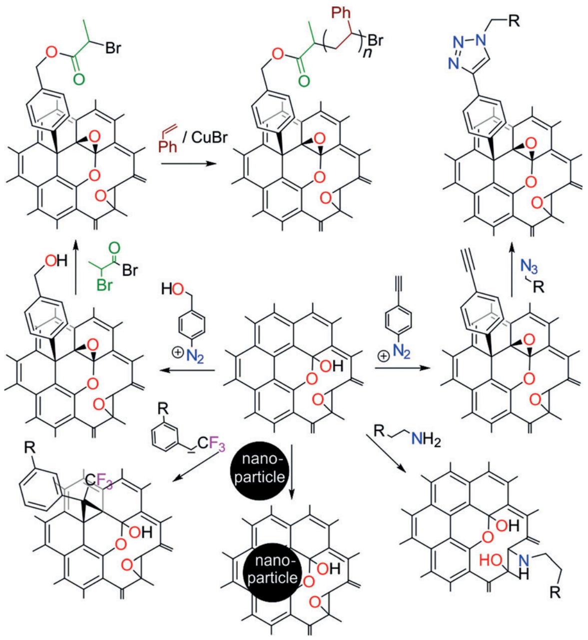

Figure 23. A selection of reactions with reduced GO bearing defects used as the starting material.

polymer composites, the diazonium salt of 2-(4-aminophenyl)ethanol was treated with reduced GO and then a subsequent atomic transfer radical polymerization reaction with methyl-2-bromopropionate enabled the grafting of styrene.[138] Furthermore, the addition of functional groups by carbene chemistry was reported.[139] Water-soluble defect-containing graphene was reported to be formed after partial reduction of GO followed by functionalization with the aryl diazonium salt of sulfanilic acid and a further reduction step.[140] Moreover, thermally exfoliated reduced GO was reported to be covalently functionalized by an amine linker with a polymer that reacts with residual epoxy groups at defect sides to form stable dispersions in tetrahydrofuran.[141] Defect-containing graphene was also stabilized by an amphiphilic coil-rod-coil conjugated triblock copolymer as the stabilizer, which contained ethylene glycol moieties and acetylene-linked phenyl groups.[77b] This composite is soluble in both organic low-polar as well as water-miscible high-polar solvents. Composites of benzylamine-reduced GO and citrate-stabilized silver nanoparticles were prepared and this composite was found to be efficient for the detection of hydrogen peroxide.[142] Hydrogen evolution was investigated using nanocomposites of TiO_2 and reduced GO as the photocatalyst.[143] Furthermore, magnetic nanocomposites of reduced GO and Fe_3O_4 were also described and are reported to be useful for the removal of arsenic.[144] The application of composites for charge storage is a popular research field, and composites of reduced GO and SnO_2, for example, are reported to perform well.[145] More examples have been recently reviewed.[15,80a]

6. Conclusions and Outlook

Most approaches for the functionalization of graphene by wet chemical methods using graphite as the starting material have so far led predominantly to the formation of derivatized few-layer graphene ($G_{<10}$-R_n), and only a few examples have been published were the formation of truly single-layer graphene derivatives G_1-R_n could be unambiguously demonstrated. The reason for this is the difficulty in accomplishing quantitative graphite exfoliation before and during the binding of the addends. Nevertheless, a large portion of the surface of the graphene layers in graphite can be targeted by binding partners if the graphite is suitably activated and exfoliated prior to the functionalization. This can be accomplished, for example, by using highly dispersible ai-GO or negatively charged graphenide as precursors. In the latter case, a pronounced electronic activation of the graphene sheets is also guaranteed, which allows for extensive redox and covalent chemistry with electron-deficient addends and electrophiles. A series of quite well-defined graphene derivatives have recently been prepared by using these approaches, and it can be expected that this field will grow substantially further.

The nomenclature of graphene- and graphite-related compounds used in the recent literature is often sloppy and misleading. As a consequence, it can be difficult and time consuming to find out what the authors are really talking about. As suggested by Koehler and Stark, a systematic nomenclature for graphene and its derivatives is desirable (Figure 24).[95d] We support such a systematic approach to nomenclature and propose a general descriptor that is applicable for many types of graphene-based systems with different sizes, defect densities, numbers of layers, and degrees of functionalization. This description will enable a substrate or an adsorbed species to also be addressed.

$$\mathrm{S}/{}^{s,d}\mathrm{G}_n - (\mathrm{R})_f\,/\mathrm{A}$$

Figure 24. S: substrate, *s*: size of graphene, *d*: structural defect density of graphene within the carbon framework, G: graphene; *n*: number of layers of graphene, R: addend, *f*: degree of functionalization, A: noncovalently bound molecules; no S: reactions applied in dispersion.[95e]

If this scheme is applied to ai-GO, a more precise descriptor would be ${}^{5\mu\mathrm{m},0.12\%}\mathrm{G}_1\text{-}[(\mathrm{OH})_x(\mathrm{O})_y(\mathrm{OSO_3H})_z]_{50\%}/(\mathrm{H_2O})_{8\%}$ and means that flakes of graphene 1 layer thick with an average flake size of 5 µm and an average defect density of about 0.12 % are functionalized on both sides with an arbitrary ratio of hydroxy, epoxy, and organosulfate groups. There is about one functional group on every second carbon atom and with 8 mass % water adsorbed. Few-layer graphene with an average size of 150 nm can be termed ${}^{150\mathrm{nm}}\mathrm{G}_{2\text{–}9}$.

Although the concepts for functionalizing graphene outlined in this Review are promising, many challenges and unsolved problems still remain. Besides controlling the size of the flakes used for functionalization, the discrimination between graphene, few-layer graphene, and graphite remains difficult. These issues also have to be addressed in future investigations to establish reliable structure–property relationships. Another important point to address is the qualitative and quantitative determination of defects within samples of graphene, few-layer graphene, and GO. Even graphene obtained by CVD methods is not necessarily free from structural defects and we want to point out that Raman spectroscopy alone is not sufficient to prove the ideality of the graphene since defects are known that do not activate the D band, as shown for zig-zag edges.[61] It is not yet fully understood to what extent silent defects activate graphene to enable chemical functionalization. In the case of GO, determination of the chemical structure is even more complex since the quantification of different oxygen addends and functional groups remains difficult. Therefore, it is not yet possible to directly determine the defect density in GO and a back conversion to reduced GO is still required to obtain this information. Furthermore, the chemical conversion of ai-GO with a very low number of impossible-to-heal σ defects has just started to emerge. The quantification of functional groups on GO is often determined by methods that are surface sensitive, but the bonding state of adsorbed impurities or reagents in many cases cannot be determined quantitatively. Therefore, new analytical approaches must be developed to qualitatively and quantitatively investigate the degree and type of functionalization in the bulk.

In the last few years, successful functionalization concepts for graphene and GO have been developed and there is no doubt that graphene can indeed be chemically converted to a large extent. In addition, GO can be functionalized without degradation of the σ framework; however, the reaction conditions must be well-controlled.

At the current level of development, the details of how the binding structure of chemically functionalized graphene affects its properties in applications are not clear. Impurities in graphene-derived compounds can play an important role; however, the exact influence has not been well addressed to date. As an example, the "metal-free" oxygen reduction of heteroatom-doped graphene can be caused by metal impurities.[146] Further fundamental investigations on G_1 derivatives are necessary to control the physical properties and to enhance the performance of graphene derivatives. Knowledge obtained from the functionalization of other synthetic carbon allotropes such as fullerenes and carbon nanotubes may be a good guide to further improve the functionalization of graphene. Only recently, the controlled synthesis of carbon nanotube derivatives by avoiding side reactions has been demonstrated.[147] Unwanted side reactions can even dominate the functionalization of graphene and should be critically discussed when considering the analytical data. Moreover, the determination of the local structure of functionalized carbon allotropes remains a challenge, and thus STM and HRTEM methods should be further developed. Another possibility for clarifying possible chemical structures is by using monodisperse organic model compounds for a given chemical conversion. In this regard, for example, oxygenated azafullerene derivatives have been studied in detail by using NMR spectroscopy and mass spectrometry.[148]

The knowledge generated by the systematic functionalization of graphene could be a very valuable basis for exploring the chemistry of other sheet materials such as MoS_2 or even so far unknown synthetic carbon allotropes. One carbon allotrope of interest is graphyne, which is composed of sp- and sp^2-hybridized carbon atoms arranged in a 2D crystal lattice.[149] Finally, applications will benefit from the controlled synthesis of graphene derivatives, and the performance of fuel cells, transparent electronics, or in vivo sensors will undoubtedly improve when defined graphene derivatives are employed. It can be expected that the full potential of graphene derivatives is not yet exploited, but the intensive collaboration of chemists, physicists, and material scientists in the future will considerably push the promising technology forward.

We thank the Deutsche Forschungsgemeinschaft (DFG-SFB 953, Project A1 "Synthetic Carbon Allotropes"; EI 938/3-1), the European Research Council (ERC; grant "246622-GRAPHENOCHEM"), and the Cluster of Excellence Engineering of Advanced Materials (EAM) for financial support. The research leading to these results has received funding from the European Union Seventh Framework Programme (grant agreement no. 604391 Graphene Flagship).

Received: February 25, 2014
Published online: June 24, 2014

---

[1] a) K. S. Novoselov, A. K. Geim, S. V. Morozov, D. Jiang, Y. Zhang, S. V. Bubonos, I. V. Grigorieva, A. A. Firsov, *Science* **2004**, *306*, 666; b) K. S. Novoselov, A. K. Geim, S. V. Morozov, D. Jiang, M. I. Katsnelson, I. V. Grigorieva, S. V. Dubonos, A. A. Firsov, *Nature* **2005**, *438*, 197; c) K. S. Novoselov, D. Jiang, F. Schedin, T. J. Booth, V. V. Khotkevich, S. V. Morozov, A. K. Geim, *Proc. Natl. Acad. Sci. USA* **2005**, *102*, 10451; d) D. R. Dreyer, R. S. Ruoff, C. W. Bielawski, *Angew. Chem.* **2010**, *122*, 9524; *Angew. Chem. Int. Ed.* **2010**, *49*, 9336; e) H.-P. Boehm, *Angew. Chem.* **2010**, *122*, 9520; *Angew. Chem. Int. Ed.* **2010**, *49*, 9332; f) S. Eigler in *Physics and Applications of Graphene—Experiments* (Ed.: S. Mikhailov), InTech, New York, **2011**, pp. 109.

[2] H. P. Boehm, A. Clauss, G. O. Fischer, U. Hofmann, *Z. Naturforsch. B* **1962**, *B17*, 150.

[3] a) M. I. Katsnelson, K. S. Novoselov, A. K. Geim, *Nat. Phys.* **2006**, *2*, 620; b) K. S. Novoselov, E. McCann, S. V. Morozov, V. I. Fal′ko, M. I. Katsnelson, U. Zeitler, D. Jiang, F. Schedin, A. K. Geim, *Nat. Phys.* **2006**, *2*, 177; c) A. K. Geim, *Angew. Chem.* **2011**, *123*, 7100; *Angew. Chem. Int. Ed.* **2011**, *50*, 6966; d) K. S. Novoselov, *Angew. Chem.* **2011**, *123*, 7123; *Angew. Chem. Int. Ed.* **2011**, *50*, 6986.

[4] a) A. H. C. Neto, N. M. R. Peres, K. S. Novoselov, A. K. Geim, *Rev. Mod. Phys.* **2009**, *81*, 109; b) C. N. Lau, W. Bao, J. Velasco, *Mater. Today* **2012**, *15*, 238.

[5] K. He, G. D. Lee, A. W. Robertson, E. Yoon, J. H. Warner, *Nat. Commun.* **2014**, *5*, 3040.

[6] a) M. J. Allen, V. C. Tung, R. B. Kaner, *Chem. Rev.* **2010**, *110*, 132; b) K. S. Novoselov, V. I. Fal′ko, L. Colombo, P. R. Gellert, M. G. Schwab, K. Kim, *Nature* **2012**, *490*, 192; c) P. Avouris, C. Dimitrakopoulos, *Mater. Today* **2012**, *15*, 86; d) R. S. Edwards, K. S. Coleman, *Nanoscale* **2013**, *5*, 38; e) D. K. James, J. M. Tour, *Acc. Chem. Res.* **2013**, *46*, 2307; f) X. Wan, Y. Huang, Y. Chen, *Acc. Chem. Res.* **2012**, *45*, 598; g) J. K. Wassei, R. B. Kaner, *Acc. Chem. Res.* **2013**, *46*, 2244.

[7] a) H. Chen, X. Guo, *Small* **2013**, *9*, 1144; b) H. Chang, H. Wu, *Adv. Funct. Mater.* **2013**, *23*, 1984; c) K. S. Kim, Y. Zhao, H. Jang, S. Y. Lee, J. M. Kim, J. H. Ahn, P. Kim, J. Y. Choi, B. H. Hong, *Nature* **2009**, *457*, 706.

[8] a) Y. Huang, J. Liang, Y. Chen, *Small* **2012**, *8*, 1805; b) J. Li, M. Östling, *Crystals* **2013**, *3*, 163.

[9] a) S. Eigler, *Carbon* **2009**, *47*, 2936; b) G. Jo, M. Choe, S. Lee, W. Park, Y. H. Kahng, T. Lee, *Nanotechnology* **2012**, *23*, 112001; c) N. O. Weiss, H. Zhou, L. Liao, Y. Liu, S. Jiang, Y. Huang, X. Duan, *Adv. Mater.* **2012**, *24*, 5782; d) X. Huang, Z. Zeng, Z. Fan, J. Liu, H. Zhang, *Adv. Mater.* **2012**, *24*, 5979; e) S. Pang, Y. Hernandez, X. Feng, K. Mullen, *Adv. Mater.* **2011**, *23*, 2779; f) P. Kumar, A. K. Singh, S. Hussain, K. N. Hui, K. S. Hui, J. Eom, J. Jung, J. Singh, *Rev. Adv. Sci. Eng.* **2013**, *2*, 238.

[10] a) D. Chen, H. Feng, J. Li, *Chem. Rev.* **2012**, *112*, 6027; b) Z. Zhu, L. Garcia-Gancedo, A. J. Flewitt, H. Xie, F. Moussy, W. I. Milne, *Sensors* **2012**, *12*, 5996; c) S. Wu, Q. He, C. Tan, Y. Wang, H. Zhang, *Small* **2013**, *9*, 1160; d) F. Schedin, A. K. Geim, S. V. Morozov, E. W. Hill, P. Blake, M. I. Katsnelson, K. S. Novoselov, *Nat. Mater.* **2007**, *6*, 652.

[11] G. Xie, K. Zhang, B. Guo, Q. Liu, L. Fang, J. R. Gong, *Adv. Mater.* **2013**, *25*, 3820.

[12] K. Lü, G. Zhao, X. Wang, *Chin. Sci. Bull.* **2012**, *57*, 1223.

[13] a) B. Luo, S. Liu, L. Zhi, *Small* **2012**, *8*, 630; b) S. Han, D. Wu, S. Li, F. Zhang, X. Feng, *Small* **2013**, *9*, 1173; c) L. Dai, *Acc. Chem. Res.* **2013**, *46*, 31; d) S. H. Hur, J.-N. Park, *Asia-Pac. J. Chem. Eng.* **2013**, *8*, 218.

[14] C. Chung, Y. K. Kim, D. Shin, S. R. Ryoo, B. H. Hong, D. H. Min, *Acc. Chem. Res.* **2013**, *46*, 2211.

[15] a) X. Sun, H. Sun, H. Li, H. Peng, *Adv. Mater.* **2013**, *25*, 5153; b) D. Wu, F. Zhang, P. Liu, X. Feng, *Chem. Eur. J.* **2011**, *17*, 10804; c) H. J. Salavagione, G. Martinez, G. Ellis, *Macromol. Rapid Commun.* **2011**, *32*, 1771; d) X. Huang, X. Qi, F. Boey, H. Zhang, *Chem. Soc. Rev.* **2012**, *41*, 666.

[16] a) A. Hirsch, M. Brettreich, *Fullerenes*, *Chemistry and Reactions*, Wiley-VCH, Weinheim, **2005**; b) A. Hirsch, *Angew. Chem.* **2002**, *114*, 1933; *Angew. Chem. Int. Ed.* **2002**, *41*, 1853; c) D. Tasis, N. Tagmatarchis, A. Bianco, M. Prato, *Chem. Rev.* **2006**, *106*, 1105.

[17] J. M. Englert, J. Röhrl, C. D. Schmidt, R. Graupner, M. Hundhausen, F. Hauke, A. Hirsch, *Adv. Mater.* **2009**, *21*, 4265.

[18] J. I. Paredes, S. Villar-Rodil, A. Martínez-Alonso, J. M. D. Tascón, *Langmuir* **2008**, *24*, 10560.

[19] N. V. Kozhemyakina, S. Eigler, R. E. Dinnebier, A. Inayat, W. Schwieger, A. Hirsch, *Fullerenes Nanotubes Carbon Nanostruct.* **2013**, *21*, 804.

[20] H. Lipson, A. R. Stokes, *Nature* **1942**, *149*, 328.

[21] S. Kurasch, J. Kotakoski, O. Lehtinen, V. Skakalova, J. Smet, C. E. Krill III, A. V. Krasheninnikov, U. Kaiser, *Nano Lett.* **2012**, *12*, 3168.

[22] A. J. Stone, D. J. Wales, *Chem. Phys. Lett.* **1986**, *128*, 501.

[23] J. Lu, Y. Bao, C. L. Su, K. P. Loh, *ACS Nano* **2013**, *7*, 8350.

[24] a) S. Park, R. S. Ruoff, *Nat. Nanotechnol.* **2009**, *4*, 217; b) Y. Zhu, S. Murali, W. Cai, X. Li, J. W. Suk, J. R. Potts, R. S. Ruoff, *Adv. Mater.* **2010**, *22*, 3906; c) D. R. Dreyer, S. Park, C. W. Bielawski, R. S. Ruoff, *Chem. Soc. Rev.* **2010**, *39*, 228.

[25] a) W. Cai, R. D. Piner, F. J. Stadermann, S. Park, M. A. Shaibat, Y. Ishii, D. Yang, A. Velamakanni, S. J. An, M. Stoller, J. An, D. Chen, R. S. Ruoff, *Science* **2008**, *321*, 1815; b) L. B. Casabianca, M. A. Shaibat, W. W. Cai, S. Park, R. Piner, R. S. Ruoff, Y. Ishii, *J. Am. Chem. Soc.* **2010**, *132*, 5672.

[26] a) S. Eigler, C. Dotzer, F. Hof, W. Bauer, A. Hirsch, *Chem. Eur. J.* **2013**, *19*, 9490; b) W. Gao, L. B. Alemany, L. Ci, P. M. Ajayan, *Nat. Chem.* **2009**, *1*, 403.

[27] R. Rozada, J. I. Paredes, S. Villar-Rodil, A. Martínez-Alonso, J. M. D. Tascón, *Nano Res.* **2013**, *6*, 216.

[28] S. Eigler, C. Dotzer, A. Hirsch, *Carbon* **2012**, *50*, 3666.

[29] S. Eigler, M. Enzelberger-Heim, S. Grimm, P. Hofmann, W. Kroener, A. Geworski, C. Dotzer, M. Rockert, J. Xiao, C. Papp, O. Lytken, H. P. Steinrück, P. Müller, A. Hirsch, *Adv. Mater.* **2013**, *25*, 3583.

[30] a) H. He, J. Klinowski, M. Forster, A. Lerf, *Chem. Phys. Lett.* **1998**, *287*, 53; b) A. Lerf, H. He, M. Forster, J. Klinowski, *J. Phys. Chem. B* **1998**, *102*, 4477.

[31] S. Eigler, Y. Hu, Y. Ishii, A. Hirsch, *Nanoscale* **2013**, *5*, 12136.

[32] B. C. Brodie, *Philos. Trans. R. Soc. London* **1859**, *149*, 249.

[33] a) L. Staudenmaier, *Ber. Dtsch. Chem. Ges.* **1898**, *31*, 1481; b) L. Staudenmaier, *Ber. Dtsch. Chem. Ges.* **1899**, *32*, 1394.

[34] J. William, S. Hummers, R. E. Offeman, *J. Am. Chem. Soc.* **1958**, *80*, 1339.

[35] A. Dimiev, D. V. Kosynkin, L. B. Alemany, P. Chaguine, J. M. Tour, *J. Am. Chem. Soc.* **2012**, *134*, 2815.

[36] K. Erickson, R. Erni, Z. Lee, N. Alem, W. Gannett, A. Zettl, *Adv. Mater.* **2010**, *22*, 4467.

[37] a) J. I. Paredes, S. Villar-Rodil, P. Solis-Fernandez, A. Martinez-Alonso, J. M. Tascon, *Langmuir* **2009**, *25*, 5957; b) K. N. Kudin, B. Ozbas, H. C. Schniepp, R. K. Prud'homme, I. A. Aksay, R. Car, *Nano Lett.* **2008**, *8*, 36.

[38] a) X. Li, W. Cai, J. An, S. Kim, J. Nah, D. Yang, R. Piner, A. Velamakanni, I. Jung, E. Tutuc, S. K. Banerjee, L. Colombo, R. S. Ruoff, *Science* **2009**, *324*, 1312; b) S. Bae, H. Kim, Y. Lee, X. Xu, J.-S. Park, Y. Zheng, J. Balakrishnan, T. Lei, H. R. Kim, Y. I. Song, Y.-J. Kim, K. S. Kim, B. Özyilmaz, J.-H. Ahn, B. H. Hong, S. Iijima, *Nat. Nanotechnol.* **2010**, *5*, 574; c) Y. Zhang, L. Zhang, C. Zhou, *Acc. Chem. Res.* **2013**, *46*, 2329; d) Y. Hao, M. S. Bharathi, L. Wang, Y. Liu, H. Chen, S. Nie, X. Wang, H. Chou, C. Tan, B. Fallahazad, H. Ramanarayan, C. W. Magnuson, E. Tutuc, B. I. Yakobson, K. F. McCarty, Y. W. Zhang, P. Kim, J. Hone, L. Colombo, R. S. Ruoff, *Science* **2013**, *342*, 720.

[39] P. Blake, E. W. Hill, A. H. C. Neto, K. S. Novoselov, D. Jiang, R. Yang, T. J. Booth, A. K. Geim, *Appl. Phys. Lett.* **2007**, *91*, 063124.

[40] a) K. V. Emtsev, A. Bostwick, K. Horn, J. Jobst, G. L. Kellogg, L. Ley, J. L. McChesney, T. Ohta, S. A. Reshanov, J. Rohrl, E. Rotenberg, A. K. Schmid, D. Waldmann, H. B. Weber, T. Seyller, *Nat. Mater.* **2009**, *8*, 203; b) B. Butz, C. Dolle, F. Niekiel, K. Weber, D. Waldmann, H. B. Weber, B. Meyer, E. Spiecker, *Nature* **2014**, *505*, 533.

[41] Q. H. Wang, Z. Jin, K. K. Kim, A. J. Hilmer, G. L. Paulus, C. J. Shih, M. H. Ham, J. D. Sanchez-Yamagishi, K. Watanabe, T. Taniguchi, J. Kong, P. Jarillo-Herrero, M. S. Strano, *Nat. Chem.* **2012**, *4*, 724.

[42] C. Schafhaeutl, *J. Prakt. Chem.* **1840**, *21*, 129.

[43] B. C. Brodie, *Ann. Chim. Phys.* **1855**, *45*, 351.

[44] L. Staudenmaier, *Ber. Dtsch. Chem. Ges.* **1899**, *32*, 2824.

[45] G. Charpy, *C. R. Hebd. Seances Acad. Sci.* **1909**, *148*, 920.

[46] W. S. Hummers, *Pereparation of graphitic acid*, US2798878, **1957**.

[47] a) M. S. Dresselhaus, G. Dresselhaus, *Adv. Phys.* **1981**, *30*, 139; b) M. S. Dresselhaus, G. Dresselhaus, *Adv. Phys.* **2002**, *51*, 1; c) A. M. Dimiev, S. M. Bachilo, R. Saito, J. M. Tour, *ACS Nano* **2012**, *6*, 7842; d) T. Enoki, M. Suzuki, M. Endo, *Graphite Intercalation Compounds and Applications*, Oxford University Press, Oxford, **2003**.

[48] S. Eigler, S. Grimm, F. Hof, A. Hirsch, *J. Mater. Chem. A* **2013**, *1*, 11559.

[49] O. C. Compton, S. W. Cranford, K. W. Putz, Z. An, L. C. Brinson, M. J. Buehler, S. T. Nguyen, *ACS Nano* **2012**, *6*, 2008.

[50] a) L. J. Cote, F. Kim, J. Huang, *J. Am. Chem. Soc.* **2009**, *131*, 1043; b) L. J. Cote, J. Kim, Z. Zhang, C. Sun, J. Huang, *Soft Matter* **2010**, *6*, 6096; c) J. W. Kim, D. Kang, T. H. Kim, S. G. Lee, N. Byun, D. W. Lee, B. H. Seo, R. S. Ruoff, H. S. Shin, *ACS Nano* **2013**, *7*, 8082.

[51] a) X. Zhou, Z. Liu, *Chem. Commun.* **2010**, *46*, 2611; b) X. Sun, D. Luo, J. Liu, D. G. Evans, *ACS Nano* **2010**, *4*, 3381; c) C.-Y. Su, Y. Xu, W. Zhang, J. Zhao, X. Tang, C.-H. Tsai, L.-J. Li, *J. Mater. Chem.* **2009**, *21*, 5674; d) Z. Luo, Y. Lu, L. A. Somers, A. T. C. Johnson, *J. Am. Chem. Soc.* **2009**, *131*, 898; e) V. C. Tung, M. J. Allen, Y. Yang, R. B. Kaner, *Nat. Nanotechnol.* **2009**, *4*, 25; f) X. Sun, Z. Liu, K. Welsher, J. T. Robinson, A. Goodwin, S. Zaric, H. Dai, *Nano Res.* **2008**, *1*, 203.

[52] S. Eigler, S. Grimm, M. Enzelberger-Heim, P. Muller, A. Hirsch, *Chem. Commun.* **2013**, *49*, 7391.

[53] a) S. Pei, H.-M. Cheng, *Carbon* **2012**, *50*, 3210; b) S. Mao, H. Pu, J. Chen, *RSC Adv.* **2012**, *2*, 2643; c) C. K. Chua, M. Pumera, *Chem. Soc. Rev.* **2014**, *43*, 291.

[54] a) A. Ganguly, S. Sharma, P. Papakonstantinou, J. Hamilton, *J. Phys. Chem. C* **2011**, *115*, 17009; b) C. Botas, P. Álvarez, P. Blanco, M. Granda, C. Blanco, R. Santamaría, L. J. Romasanta, R. Verdejo, M. A. López-Manchado, R. Menéndez, *Carbon* **2013**, *65*, 156.

[55] M. Z. Hossain, J. E. Johns, K. H. Bevan, H. J. Karmel, Y. T. Liang, S. Yoshimoto, K. Mukai, T. Koitaya, J. Yoshinobu, M. Kawai, A. M. Lear, L. L. Kesmodel, S. L. Tait, M. C. Hersam, *Nat. Chem.* **2012**, *4*, 305.

[56] a) Y. Liang, J. Frisch, L. Zhi, H. Norouzi-Arasi, X. Feng, J. P. Rabe, N. Koch, K. Müllen, *Nanotechnology* **2009**, *20*, 434007; b) V. López, R. S. Sundaram, C. Gómez-Navarro, D. Olea, M. Burghard, J. Gómez-Herrero, F. Zamora, K. Kern, *Adv. Mater.* **2009**, *21*, 4683; c) S. Some, Y. Kim, Y. Yoon, H. Yoo, S. Lee, Y. Park, H. Lee, *Sci. Rep.* **2013**, *3*, 1929.

[57] C. Gómez-Navarro, J. C. Meyer, R. S. Sundaram, A. Chuvilin, S. Kurasch, M. Burghard, K. Kern, U. Kaiser, *Nano Lett.* **2010**, *10*, 1144.

[58] S. Park, Y. Hu, J. O. Hwang, E.-S. Lee, L. B. Casabianca, W. Cai, J. R. Potts, H.-W. Ha, S. Chen, J. Oh, S. O. Kim, Y.-H. Kim, Y. Ishii, R. S. Ruoff, *Nat. Commun.* **2012**, *3*, 638.

[59] S. Fujii, T. Enoki, *ACS Nano* **2013**, *7*, 11190.

[60] a) J. M. Englert, P. Vecera, K. C. Knirsch, R. A. Schafer, F. Hauke, A. Hirsch, *ACS Nano* **2013**, *7*, 5472; b) S. Eigler, F. Hof, M. Enzelberger-Heim, S. Grimm, P. Müller, A. Hirsch, *J. Phys. Chem. C* **2014**, *118*, 7698–7704.

[61] A. C. Ferrari, D. M. Basko, *Nat. Nanotechnol.* **2013**, *8*, 235.

[62] a) L. G. Cançado, A. Jorio, E. H. M. Ferreira, F. Stavale, C. A. Achete, R. B. Capaz, M. V. O. Moutinho, A. Lombardo, T. S. Kulmala, A. C. Ferrari, *Nano Lett.* **2011**, *11*, 3190; b) M. M. Lucchese, F. Stavale, E. H. M. Ferreira, C. Vilani, M. V. O. Moutinho, R. B. Capaz, C. A. Achete, A. Jorio, *Carbon* **2010**, *48*, 1592.

[63] J. M. Englert, C. Dotzer, G. Yang, M. Schmid, C. Papp, J. M. Gottfried, H.-P. Steinrück, E. Spiecker, F. Hauke, A. Hirsch, *Nat. Chem.* **2011**, *3*, 279.

[64] a) A. K. Geim, K. S. Novoselov, *Nat. Mater.* **2007**, *6*, 183; b) A. K. Geim, *Science* **2009**, *324*, 1530; c) G. Ruan, Z. Sun, Z. Peng, J. M. Tour, *ACS Nano* **2011**, *5*, 7601.

[65] W. Norimatsu, M. Kusunoki, *Phys. Chem. Chem. Phys.* **2014**, *16*, 3501.

[66] G. Cravotto, P. Cintas, *Chem. Eur. J.* **2010**, *16*, 5246.

[67] A. Ciesielski, P. Samorì, *Chem. Soc. Rev.* **2014**, *43*, 381.

[68] a) F. Bonaccorso, A. Lombardo, T. Hasan, Z. Sun, L. Colombo, A. C. Ferrari, *Mater. Today* **2012**, *15*, 564; b) J. N. Coleman, *Acc. Chem. Res.* **2013**, *46*, 14.

[69] a) I. Y. Jeon, H. J. Choi, S. M. Jung, J. M. Seo, M. J. Kim, L. Dai, J. B. Baek, *J. Am. Chem. Soc.* **2013**, *135*, 1386; b) V. León, M. Quintana, M. A. Herrero, J. L. Fierro, A. de La Hoz, M. Prato, E. Vázquez, *Chem. Commun.* **2011**, *47*, 10936; c) M. Lotya, Y. Hernandez, P. J. King, R. J. Smith, V. Nicolosi, L. S. Karlsson, F. M. Blighe, S. De, Z. Wang, I. T. McGovern, G. S. Duesberg, J. N. Coleman, *J. Am. Chem. Soc.* **2009**, *131*, 3611; d) J. N. Coleman, *Adv. Funct. Mater.* **2009**, *19*, 3680.

[70] a) A. A. Green, M. C. Hersam, *Nano Lett.* **2009**, *9*, 4031; b) A. A. Green, M. C. Hersam, *J. Phys. Chem. Lett.* **2010**, *1*, 544.

[71] J. Chattopadhyay, A. Mukherjee, S. Chakraborty, J. Kang, P. J. Loos, K. F. Kelly, H. K. Schmidt, W. E. Billups, *Carbon* **2009**, *47*, 2945.

[72] a) E. M. Milner, N. T. Skipper, C. A. Howard, M. S. Shaffer, D. J. Buckley, K. A. Rahnejat, P. L. Cullen, R. K. Heenan, P. Lindner, R. Schweins, *J. Am. Chem. Soc.* **2012**, *134*, 8302; b) A. Pénicaud, C. Drummond, *Acc. Chem. Res.* **2013**, *46*, 129.

[73] C. Vallés, C. Drummond, H. Saadaoui, C. A. Furtado, M. He, O. Roubeau, L. Ortolani, M. Monthioux, A. Pénicaud, *J. Am. Chem. Soc.* **2008**, *130*, 15802.

[74] S. R. Dhakate, N. Chauhan, S. Sharma, J. Tawale, S. Singh, P. D. Sahare, R. B. Mathur, *Carbon* **2011**, *49*, 1946.

[75] X. Liu, J. Liu, D. Zhan, J. Yan, J. Wang, D. Chao, L. Lai, M. Chen, J. Yin, Z. Shen, *RSC Adv.* **2013**, *3*, 11601.

[76] J. Zheng, C. A. Di, Y. Liu, H. Liu, Y. Guo, C. Du, T. Wu, G. Yu, D. Zhu, *Chem. Commun.* **2010**, *46*, 5728.

[77] a) Y. Xu, H. Bai, G. Lu, C. Li, G. Shi, *J. Am. Chem. Soc.* **2008**, *130*, 5856; b) X. Qi, K. Y. Pu, H. Li, X. Zhou, S. Wu, Q. L. Fan, B. Liu, F. Boey, W. Huang, H. Zhang, *Angew. Chem.* **2010**, *122*, 9616; *Angew. Chem. Int. Ed.* **2010**, *49*, 9426.

[78] S. Some, Y. Kim, E. Hwang, H. Yoo, H. Lee, *Chem. Commun.* **2012**, *48*, 7732.

[79] K. Parvez, R. Li, S. R. Puniredd, Y. Hernandez, F. Hinkel, S. Wang, X. Feng, K. Mullen, *ACS Nano* **2013**, *7*, 3598.

[80] a) V. Georgakilas, M. Otyepka, A. B. Bourlinos, V. Chandra, N. Kim, K. C. Kemp, P. Hobza, R. Zboril, K. S. Kim, *Chem. Rev.* **2012**, *112*, 6156; b) S. P. Economopoulos, N. Tagmatarchis, *Chem. Eur. J.* **2013**, *19*, 12930; c) Q. Tang, Z. Zhou, Z. Chen, *Nanoscale* **2013**, *5*, 4541.

[81] Q. Su, S. Pang, V. Alijani, C. Li, X. Feng, K. Müllen, *Adv. Mater.* **2009**, *21*, 3191.

[82] M. Lotya, P. J. King, U. Khan, S. De, J. N. Coleman, *ACS Nano* **2010**, *4*, 3155.

[83] S. Vadukumpully, J. Paul, S. Valiyaveettil, *Carbon* **2009**, *47*, 3288.

[84] A. S. Wajid, S. Das, F. Irin, H. S. T. Ahmed, J. L. Shelburne, D. Parviz, R. J. Fullerton, A. F. Jankowski, R. C. Hedden, M. J. Green, *Carbon* **2012**, *50*, 526.

[85] S. Das, F. Irin, H. S. T. Ahmed, A. B. Cortinas, A. S. Wajid, D. Parviz, A. F. Jankowski, M. Kato, M. J. Green, *Polymer* **2012**, *53*, 2485.

[86] D. Parviz, S. Das, H. S. Ahmed, F. Irin, S. Bhattacharia, M. J. Green, *ACS Nano* **2012**, *6*, 8857.

[87] A. Ghosh, K. V. Rao, S. J. George, C. N. Rao, *Chem. Eur. J.* **2010**, *16*, 2700.

[88] N. V. Kozhemyakina, J. M. Englert, G. Yang, E. Spiecker, C. D. Schmidt, F. Hauke, A. Hirsch, *Adv. Mater.* **2010**, *22*, 5483.

[89] D. E. Jiang, B. G. Sumpter, S. Dai, *J. Phys. Chem. B* **2006**, *110*, 23628.

[90] a) H. X. Wang, Q. Wang, K. G. Zhou, H. L. Zhang, *Small* **2013**, *9*, 1266; b) J. Park, M. Yan, *Acc. Chem. Res.* **2013**, *46*, 181; c) A. Hirsch, J. M. Englert, F. Hauke, *Acc. Chem. Res.* **2013**, *46*, 87; d) M. Quintana, E. Vazquez, M. Prato, *Acc. Chem. Res.* **2013**, *46*, 138; e) L. H. Liu, M. M. Lerner, M. Yan, *Nano Lett.* **2010**, *10*, 3754.

[91] M. Pumera, C. H. Wong, *Chem. Soc. Rev.* **2013**, *42*, 5987.

[92] J. T. Robinson, J. S. Burgess, C. E. Junkermeier, S. C. Badescu, T. L. Reinecke, F. K. Perkins, M. K. Zalalutdniov, J. W. Baldwin, J. C. Culbertson, P. E. Sheehan, E. S. Snow, *Nano Lett.* **2010**, *10*, 3001.

[93] a) D. C. Elias, R. R. Nair, T. M. Mohiuddin, S. V. Morozov, P. Blake, M. P. Halsall, A. C. Ferrari, D. W. Boukhvalov, M. I. Katsnelson, A. K. Geim, K. S. Novoselov, *Science* **2009**, *323*, 610; b) H. Gao, L. Wang, J. Zhao, F. Ding, J. Lu, *J. Phys. Chem. C* **2011**, *115*, 3236; c) R. A. Schäfer, J. M. Englert, P. Wehrfritz, W. Bauer, F. Hauke, T. Seyller, A. Hirsch, *Angew. Chem.* **2013**, *125*, 782; *Angew. Chem. Int. Ed.* **2013**, *52*, 754; d) R. R. Nair, W. Ren, R. Jalil, I. Riaz, V. G. Kravets, L. Britnell, P. Blake, F. Schedin, A. S. Mayorov, S. Yuan, M. I. Katsnelson, H. M. Cheng, W. Strupinski, L. G. Bulusheva, A. V. Okotrub, I. V. Grigorieva, A. N. Grigorenko, K. S. Novoselov, A. K. Geim, *Small* **2010**, *6*, 2877; e) F. Karlicky, R. Zboril, M. Otyepka, *J. Chem. Phys.* **2012**, *137*, 034709; f) R. Zboril, F. Karlicky, A. B. Bourlinos, T. A. Steriotis, A. K. Stubos, V. Georgakilas, K. Safarova, D. Jancik, C. Trapalis, M. Otyepka, *Small* **2010**, *6*, 2885; g) J. E. Johns, M. C. Hersam, *Acc. Chem. Res.* **2013**, *46*, 77; h) Z. Yang, Y. Sun, L. B. Alemany, T. N. Narayanan, W. E. Billups, *J. Am. Chem. Soc.* **2012**, *134*, 18689.

[94] F. M. Koehler, A. Jacobsen, K. Ensslin, C. Stampfer, W. J. Stark, *Small* **2010**, *6*, 1125.

[95] a) E. Bekyarova, S. Sarkar, S. Niyogi, M. E. Itkis, R. C. Haddon, *J. Phys. D* **2012**, *45*, 154009; b) S. Niyogi, E. Bekyarova, M. E. Itkis, H. Zhang, K. Shepperd, J. Hicks, M. Sprinkle, C. Berger, C. N. Lau, W. A. deHeer, E. H. Conrad, R. C. Haddon, *Nano Lett.* **2010**, *10*, 4061; c) F. M. Koehler, N. A. Luechinger, D. Ziegler, E. K. Athanassiou, R. N. Grass, A. Rossi, C. Hierold, A. Stemmer, W. J. Stark, *Angew. Chem.* **2009**, *121*, 230; *Angew. Chem. Int. Ed.* **2009**, *48*, 224; d) F. M. Koehler, W. J. Stark, *Acc. Chem. Res.* **2013**, *46*, 2297.

[96] a) R. Sharma, J. H. Baik, C. J. Perera, M. S. Strano, *Nano Lett.* **2010**, *10*, 398; b) E. Bekyarova, M. E. Itkis, P. Ramesh, C. Berger, M. Sprinkle, W. A. de Heer, R. C. Haddon, *J. Am. Chem. Soc.* **2009**, *131*, 1336.

[97] H. Lim, J. S. Lee, H. J. Shin, H. S. Shin, H. C. Choi, *Langmuir* **2010**, *26*, 12278.

[98] Q. Wu, Y. Wu, Y. Hao, J. Geng, M. Charlton, S. Chen, Y. Ren, H. Ji, H. Li, D. W. Boukhvalov, R. D. Piner, C. W. Bielawski, R. S. Ruoff, *Chem. Commun.* **2013**, *49*, 677.

[99] H. Liu, S. Ryu, Z. Chen, M. L. Steigerwald, C. Nuckolls, L. E. Brus, *J. Am. Chem. Soc.* **2009**, *131*, 17099.

[100] L. Rodríguez-Pérez, M. Á. Herranz, N. Martín, *Chem. Commun.* **2013**, *49*, 3721.

[101] C. E. Hamilton, J. R. Lomeda, Z. Sun, J. M. Tour, A. R. Barron, *Nano Lett.* **2009**, *9*, 3460.

[102] Z. Jin, T. P. McNicholas, C.-J. Shih, Q. H. Wang, G. L. C. Paulus, A. J. Hilmer, S. Shimizu, M. S. Strano, *Chem. Mater.* **2011**, *23*, 3362.

[103] M. Quintana, K. Spyrou, M. Grzelczak, W. R. Browne, P. Rudolf, M. Prato, *ACS Nano* **2010**, *4*, 3527.

[104] X. Zhong, J. Jin, S. Li, Z. Niu, W. Hu, R. Li, J. Ma, *Chem. Commun.* **2010**, *46*, 7340.

[105] C. K. Chua, A. Ambrosi, M. Pumera, *Chem. Commun.* **2012**, *48*, 5376.

[106] S. Sarkar, E. Bekyarova, S. Niyogi, R. C. Haddon, *J. Am. Chem. Soc.* **2011**, *133*, 3324.

[107] E. K. Choi, I. Y. Jeon, S. Y. Bae, H. J. Lee, H. S. Shin, L. Dai, J. B. Baek, *Chem. Commun.* **2010**, *46*, 6320.

[108] H. X. Wang, K. G. Zhou, Y. L. Xie, J. Zeng, N. N. Chai, J. Li, H. L. Zhang, *Chem. Commun.* **2011**, *47*, 5747.

[109] K. S. Subrahmanyam, P. Kumar, U. Maitra, A. Govindaraj, K. P. Hembram, U. V. Waghmare, C. N. Rao, *Proc. Natl. Acad. Sci. USA* **2011**, *108*, 2674.

[110] V. A. Nalimova, D. Guérard, M. Lelaurain, O. V. Fateev, *Carbon* **1995**, *33*, 177.

[111] a) C. Vallés, C. Drummond, H. Saadaoui, C. A. Furtado, M. He, O. Roubeau, L. Ortolani, M. Monthioux, A. Pénicaud, *J. Am. Chem. Soc.* **2008**, *130*, 15802; b) K. F. Kelly, W. E. Billups, *Acc. Chem. Res.* **2013**, *46*, 4.

[112] J. M. Englert, K. C. Knirsch, C. Dotzer, B. Butz, F. Hauke, E. Spiecker, A. Hirsch, *Chem. Commun.* **2012**, *48*, 5025.

[113] a) G. L. Paulus, Q. H. Wang, M. S. Strano, *Acc. Chem. Res.* **2013**, *46*, 160; b) X. Y. Fan, R. Nouchi, L. C. Yin, K. Tanigaki, *Nanotechnology* **2010**, *21*, 475208.

[114] S. Kim, S. Zhou, Y. Hu, M. Acik, Y. J. Chabal, C. Berger, W. de Heer, A. Bongiorno, E. Riedo, *Nat. Mater.* **2012**, *11*, 544.

[115] S. Eigler, C. Dotzer, A. Hirsch, M. Enzelberger, P. Müller, *Chem. Mater.* **2012**, *24*, 1276.

[116] A. M. Dimiev, L. B. Alemany, J. M. Tour, *ACS Nano* **2013**, *7*, 576.

[117] T. H. Han, Y. K. Huang, A. T. Tan, V. P. Dravid, J. Huang, *J. Am. Chem. Soc.* **2011**, *133*, 15264.

[118] Y. Zhu, S. Murali, M. D. Stoller, K. J. Ganesh, W. Cai, P. J. Ferreira, A. Pirkle, R. M. Wallace, K. A. Cychosz, M. Thommes, D. Su, E. A. Stach, R. S. Ruoff, *Science* **2011**, *332*, 1537.

[119] P. Montes-Navajas, N. G. Asenjo, R. Santamaría, R. Menéndez, A. Corma, H. García, *Langmuir* **2013**, *29*, 13443.

[120] Z. Liu, J. T. Robinson, X. Sun, H. Dai, *J. Am. Chem. Soc.* **2008**, *130*, 10876.

[121] a) X. Zhang, Y. Huang, Y. Wang, Y. Ma, Z. Liu, Y. Chen, *Carbon* **2009**, *47*, 334; b) Y. Xu, Z. Liu, X. Zhang, Y. Wang, J. Tian, Y. Huang, Y. Ma, X. Zhang, Y. Chen, *Adv. Mater.* **2009**, *21*, 1275; c) D. Yu, Y. Yang, M. Durstock, J. B. Baek, L. Dai, *ACS Nano* **2010**, *4*, 5633.

[122] a) A. B. Bourlinos, D. Gournis, D. Petridis, T. Szabó, A. Szeri, I. Dékány, *Langmuir* **2003**, *19*, 6050; b) H. Yang, C. Shan, F. Li, D. Han, Q. Zhang, L. Niu, *Chem. Commun.* **2009**, 3880.

[123] a) J. Kim, L. J. Cote, J. Huang, *Acc. Chem. Res.* **2012**, *45*, 1356; b) K. P. Loh, Q. Bao, P. K. Ang, J. Yang, *J. Mater. Chem.* **2010**, *20*, 2277; c) T. Kuila, S. Bose, A. K. Mishra, P. Khanra, N. H. Kim, J. H. Lee, *Prog. Mater. Sci.* **2012**, *57*, 1061.

[124] a) H. Hu, Z. Zhao, W. Wan, Y. Gogotsi, J. Qiu, *Adv. Mater.* **2013**, *25*, 2219; b) H. Sun, Z. Xu, C. Gao, *Adv. Mater.* **2013**, *25*, 2554.

[125] J. W. Burress, S. Gadipelli, J. Ford, J. M. Simmons, W. Zhou, T. Yildirim, *Angew. Chem.* **2010**, *122*, 9086; *Angew. Chem. Int. Ed.* **2010**, *49*, 8902.

[126] S. Stankovich, R. D. Piner, S. T. Nguyen, R. S. Ruoff, *Carbon* **2006**, *44*, 3342.

[127] J. Wang, M. Liang, Y. Fang, T. Qiu, J. Zhang, L. Zhi, *Adv. Mater.* **2012**, *24*, 2874.

[128] L. J. Cote, J. Kim, V. C. Tung, J. Luo, F. Kim, J. Huang, *Pure Appl. Chem.* **2011**, *83*, 95.

[129] W. Zhang, Z. Guo, D. Huang, Z. Liu, X. Guo, H. Zhong, *Biomaterials* **2011**, *32*, 8555.

[130] C. H. Lu, H. H. Yang, C. L. Zhu, X. Chen, G. N. Chen, *Angew. Chem.* **2009**, *121*, 4879; *Angew. Chem. Int. Ed.* **2009**, *48*, 4785.

[131] S. Borini, R. White, D. Wei, M. Astley, S. Haque, E. Spigone, N. Harris, J. Kivioja, T. Ryhanen, *ACS Nano* **2013**, *7*, 11166.

[132] J. Liu, M. Durstock, L. Dai, *Energy Environ. Sci.* **2014**, *7*, 1297–1306.

[133] F. Beckert, A. M. Rostas, R. Thomann, S. Weber, E. Schleicher, C. Friedrich, R. Mülhaupt, *Macromolecules* **2013**, *46*, 5488.

[134] a) H. He, C. Gao, *Chem. Mater.* **2010**, *22*, 5054; b) S. Stankovich, D. A. Dikin, G. H. Dommett, K. M. Kohlhaas, E. J. Zimney, E. A. Stach, R. D. Piner, S. T. Nguyen, R. S. Ruoff, *Nature* **2006**, *442*, 282.

[135] X. Yang, C. Cheng, Y. Wang, L. Qiu, D. Li, *Science* **2013**, *341*, 534.

[136] S. Eigler, S. Grimm, A. Hirsch, *Chem. Eur. J.* **2014**, *20*, 984.

[137] a) M. Castelaín, G. Martínez, P. Merino, J. Á. Martín-Gago, J. L. Segura, G. Ellis, H. J. Salavagione, *Chem. Eur. J.* **2012**, *18*, 4965; b) J. R. Lomeda, C. D. Doyle, D. V. Kosynkin, W.-F. Hwang, J. M. Tour, *J. Am. Chem. Soc.* **2008**, *130*, 16201.

[138] M. Fang, K. Wang, H. Lu, Y. Yang, S. Nutt, *J. Mater. Chem.* **2010**, *20*, 1982.

[139] H. Ismaili, D. Geng, A. X. Sun, T. T. Kantzas, M. S. Workentin, *Langmuir* **2011**, *27*, 13261.

[140] Y. Si, E. T. Samulski, *Nano Lett.* **2008**, *8*, 1679.

[141] M. C. Hsiao, S. H. Liao, M. Y. Yen, P. I. Liu, N. W. Pu, C. A. Wang, C. C. Ma, *ACS Appl. Mater. Interfaces* **2010**, *2*, 3092.

[142] S. Liu, J. Tian, L. Wang, X. Sun, *Carbon* **2011**, *49*, 3158.

[143] W. Fan, Q. Lai, Q. Zhang, Y. Wang, *J. Phys. Chem. C* **2011**, *115*, 10694.

[144] V. Chandra, J. Park, Y. Chun, J. W. Lee, I. C. Hwang, K. S. Kim, *ACS Nano* **2010**, *4*, 3979.

[145] L.-S. Zhang, L.-Y. Jiang, H.-J. Yan, W. D. Wang, W. Wang, W.-G. Song, Y.-G. Guo, L.-J. Wan, *J. Mater. Chem.* **2010**, *20*, 5462.

[146] L. Wang, A. Ambrosi, M. Pumera, *Angew. Chem.* **2013**, *125*, 14063; *Angew. Chem. Int. Ed.* **2013**, *52*, 13818.

[147] F. Hof, S. Bosch, S. Eigler, F. Hauke, A. Hirsch, *J. Am. Chem. Soc.* **2013**, *135*, 18385.

[148] R. Eigler, F. W. Heinemann, A. Hirsch, *Chem. Commun.* **2014**, *50*, 2021.

[149] D. Malko, C. Neiss, F. Viñes, A. Görling, *Phys. Rev. Lett.* **2012**, *108*, 086804.